~~SECRET / H~~

7-1779-74
BIF003W/2-091480-74
HEXAGON
Sheet Count: 90
Copy: 18

CONTRACT ~~(S)~~

SV-8 FLIGHT TEST SOLO REPORT ~~(S)~~

8 NOVEMBER 1974

Prepared and Submitted by SBAC

J. W. Chapman

JWC:RTK:jlb

CLASSIFIED BY BYEMAN 1 EXEMPT FROM GENERAL DECLASSIFICATION SCHEDULE OF E.O. 11652, EXEMPTION CATEGORY: 5B, (2) AUTOMATICALLY DECLASSIFIED ON: IMPOSSIBLE TO DETERMINE	NATIONAL SECURITY INFORMATION UNAUTHORIZED DISCLOSURE SUBJECT TO CRIMINAL SANCTIONS WARNING NOTICE SENSITIVE INTELLIGENCE SOURCES AND METHODS INVOLVED	HANDLE VIA BYEMAN CONTROL SYSTEM ONLY

~~SECRET / H~~

FOREWORD

This report describes the solo testing as authorized by the "Solo Plan for Flight Vehicle 8" and its supplements. It is issued in compliance with CDRL Sequence A001AW of Contract [redacted]

TABLE OF CONTENTS

TABLE OF CONTENTS (Continued)

LIST OF ILLUSTRATIONS

LIST OF TABLES

1.0 INTRODUCTION

1.1 General

SV-8 is the eighth in a series of vehicles launched for the HEXAGON Program. Its launch configuration consisted of a primary payload which included a camera system (SSC) with 4 recovery vehicles (MWC), a secondary payload which included a Terrain Camera plus two Stellar Cameras (NEC) with one Recovery Vehicle (OPC), and four Tertiary Payloads which included the [redacted] -Y Subsatellite (SSU), +Y Subsatellite [redacted] and a Quantic Horizon Sensor and Star Tracker System (Quantic Experiment).

The planned orbital activities for SV-8 consisted of two phases. Phase I, the primary photographic mission, extended through Day 106 with success in all primary objectives. Phase II, the Solo Phase continued through Day 110 and was used principally for conducting Quantic experiments. It should be pointed out that some Solo Tests were accomplished during Phase I on a non-interference basis.

1.2 SV-8 Flight History

Operations for the primary photographic mission and Solo testing were completed as follows:

Event	Rev	Day	Date
Launch	---	1	10 April 1974
+Y Subsatellite Separation	3	1	10 April 1974
-Y Subsatellite Separation	13	1	10 April 1974
RV 1 Recovery	228	15	24 April 1974
RV 2 Recovery	681	43	22 May 1974
RV 5 Recovery	973	60	9 June 1974
RV 3 Recovery	1118	70	18 June 1974
RV 4 Recovery	1701	106	24 July 1974
Solo Start	1701	106	24 July 1974
Solo Complete (Deboost)	1768	110	28 July 1974

1.3 Summary of SV-8 Solo Activity

Solo testing started in a limited way after completion of the Stellar Terrain Subsystem mission on the tests that could be conducted without impacting the primary mission. Full Solo testing started after RV 4 recovery on Rev 1701. All activities were successfully completed, including deboost on Rev 1768. The chronology of Solo testing went as follows:

Rev	Solo ID	Event
Completion of ST Mission/RV-5 Recovery Rev 973		
1004 - 1053	OPS-1 (n, o)	DBS Redundant Oscillator and Heater
RV-3 Recovery, Rev 1118		
1200	Q-10A	1 rev inertial hold.
1200	EDAP-1	Solar Array Albedo-Inertial
1200	THERM-1	Sun Exposure
1327	OPS-1 (c - g)	Operation with Redundant Servo Electronics
1344 - 1345	ST-5	Operation with one Coverter off
1361	ST-4	± Stellar Capping Shutter
1361	ST-2, ST-3	FA Open at 10% and 78% overlap.
1376 - 1378	Q-11	Pylon and SV Attitude Estimation
1458	ST-1	Thermal Shutter Emergency Open
1466	OPS-2 (a)	Backup Timer
1470	Q-2	H/S Pitch Bias Check
1473 - 1474	Q-11	Pylon and SV Attitude Estimation
1477	ST-1	Thermal Shutter Emergency Open
1539	TTC-3	SGLS 2
1540	TTC-3	SGLS 2
1555	Q-2	H/S Pitch Bias Check
1571	TTC-3	SGLS 2
1588	TTC-3	SGLS 2
1633	Q-16	Pitch Maneuver Calibration
1635 - 1637	Q-11	Pylon and SV Attitude Estimation
1669 - 1685	OPS-1 (j)	Redundant TCEA
1697	RX-1	Pan Camera Pneumatic - RV-4 ATC

Rev	Solo ID	Event
RV-4 Recovery - Rev 1701 - Start Solo		
1704	Q-9	OA Environment
1704	Q-22	Sequential Maneuver Calibration
1705 - 1706	Q-16	Roll Maneuver Calibration
1707 - 1718	Q-13	Low Frequency Horizon Radiance
1710	TTC-2	PCM RU 4A with MUX 2
1714 - 1715	Q-17B	Pitch H/S Inhibit
1715 - 1717	Q-11	Pylon and SV Attitude Estimation
1718	Q-20B	Sun Impingement
1720 - 1723	Q-10B	Pitch Roll Gyro Drift Calibration
1724 - 1726	EDAP-2	Solar Array Output - Albedo-Geocentric
1729 - 1731	EDAP-4	Solar Array Output - End to Earth
1733 - 1735	Q-24	Geocentric Rate Determination
1734 - 1735	OPS-2 (e, f, f, h)	Redundant OAS/RCS Tank Heaters
1735	OPS-1 (f)	Lifeboat Tank Heaters
1738 - 1739	OPS-1 (g, h,i)	Primary OAS and RCS Tank Heater
1738 - 1739	Q-17A	Roll Horizon Sensor Inhibit
1739 - 1741	RCS-1	RCS-1 Storage Effects
1742 - 1745	EDAP-5	Solar Array Output - End to Sun
1747	Q-23	Gyro Reference Plane Calibration
1749 - 1750	Q-25	Star Tracker 1 Health Check
1751 - 1752	Q-21	Lifeboat Attitude Estimation
1751 - 1752	OPS-1(e)	Lifeboat Execute
1753 - 1768	THERM-2	Fly Reverse (-30° Beta)
1753	ACS-2	PACS Thermal Cycle - Off
1754 - 1755	OPS-1(a)	SGLS 2 Performance
1756 - 1758	Q-11	Pylon and SV Attitude Estimation
1757	TTC-1	SGLS 1 Frequency Measurement
1757	ACS-1	Solar Array Dynamics
1760	ACS-2	PACS Thermal Cycle - On

Rev	Solo ID	Event
RV-4 Recovery - Rev 1701 - Start Solo (Continued)		
1762 - 1765	Q-18	Best Bet Attitude
1765	---	Star Tracker 1 On
1768	OAS-1	Burn to Depletion
1768	---	Deboost

2.0 SOLO TESTS - SBAC

2.1 ACS-1, Solar Array Dynamics

Rationale

The structural damping associated with Solar Arrays extended is an important parameter in defining control gas usage rates. Successful damping tests were made on SV-1, SV-4 and SV-7. A repeat of the test was to provide an additional sample of structural damping and frequency characteristics.

Procedure

Roll the vehicle in a negative direction for 5.0 seconds. Ten seconds after removal of the negative roll rate command, roll the vehicle in a positive direction for 5.0 seconds. About twenty-five (25) seconds after removal of the positive roll rate command, disable the ACS 2 control for approximately 150 seconds. Obtain tape recorder data for duration of test plus 300 seconds.

Results

A Solar Array Dynamic Test was run on Rev 1757.9 with M2V2 the controlling system. The maneuver durations and the coast duration of the sequence were chosen so that the primary solar array bending mode of 0.1 Hz would be excited. After allowing 24.8 seconds for control stabilization, the thruster power was removed and the vehicle was allowed to go without control for 150.2 seconds.

It was during the non-controlled portion of the experiment that the roll rate decay was observed and from which the damping was calculated. The sequence used in this test was as follows:

Command	System Time	Vehicle Time
H/S 2 DISC	26794.8	143792.4
FDU-	26794.9	143792.6
FINE MODE, GEO-	26795.1	143792.8
GYR-	26795.3	143793.0
ROLL NEG	26795.8	143793.4
STOP ROLL	26800.8	143798.4
ROLL POS	26810.8	143808.4

Command	System Time	Vehicle Time
STOP ROLL	26815.8	143813.4
ACS2-	26840.5	143838.2
ACS2 ENA	26840.9	143838.6
IRA2 ACT	26841.1	143838.8
ACS MST CLR 2-	26841.5	143839.2
H/S 2 CONN	26841.9	143839.6
COARSE MODE, GEO+	26988.8	143986.4
FLY FWD, GYR+	26989.8	143987.4
FLY REV, GYR+	26990.1	143987.8
ACS 2 EXECUTE	26990.8	143988.4
FDU+	27025.8	144023.4
FINE MODE	27105.8	144103.4

As shown in Figure 1, the average roll rate during the non-controlled portion of the experiment was +0.10 degrees/second. The roll H/S of ACS 2 inhibited at 143840.8 seconds vehicle time, but was non-inhibited again at 143898.8 seconds vehicle time.

On the next rev (1758.3), the vehicle was stabilized and was flying in Fine Mode (M2V2). The following conclusions were drawn from analysis of the data:

(1) The cantilevered frequency of the array is 0.1 Hz, confirming results obtained from SV-1, SV-4 and SV-7 tests.

(2) The SV-8 roll response shows a beating phenomena which is indicative of nonsymmetries in the system. These nonsymmetries result in array modes in which the SV response is not simply in the pitch plane or about the roll axis but some combination of response in the pitch plane and about the roll axis. This coupled motion effect makes it more difficult to excite the array mode which has the dominant roll motion without also exciting the mode which has the dominant pitch component of the SV.

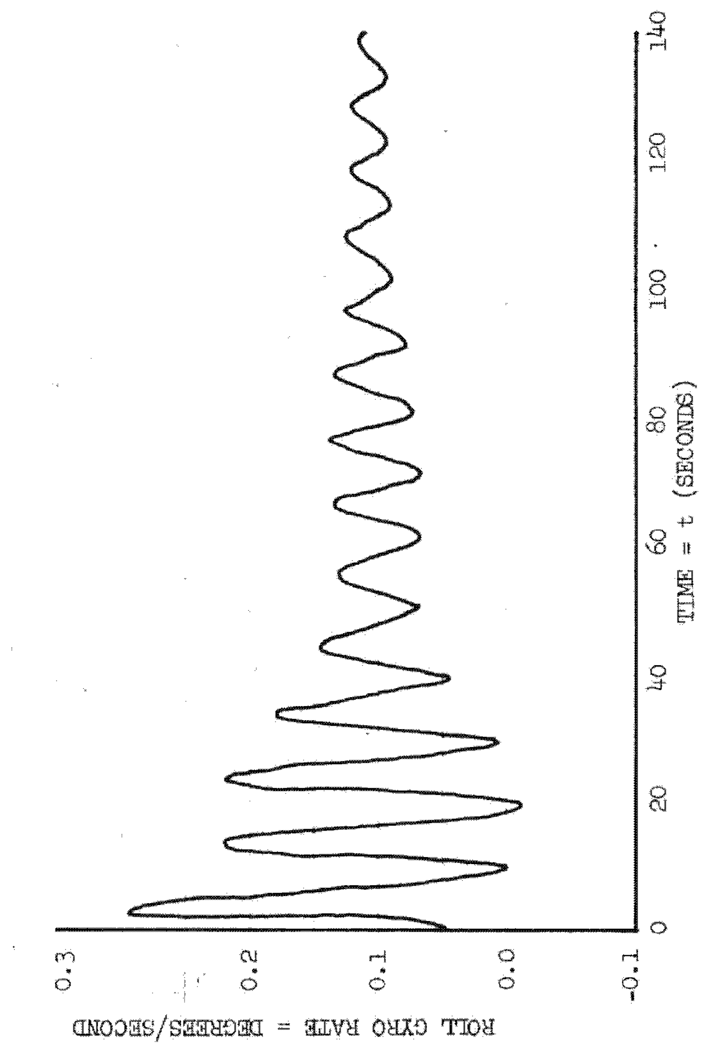

Figure 1
Solar Array Dynamic Test - Roll Rate Response

(3) Even with the slight beating phenomena, it is possible to conclude that the dominant roll mode is damped slightly higher than 3.0 percent critical. SV-7, which had a very clean roll response in the array test, also gave a damping value greater than 3.0 percent critical.

2.2 ACS-2, PACS Thermal Cycle

Rationale

Two anomalous conditions were noted in ACS performance during the primary mission. A noise problem was evident on the PACS Roll Channel Gyro, Serial Number 1021, and unexpected transients occurred on the PACS HSA, Serial Number 1007. The purpose of this Solo experiment was to determine if either or both of these conditions could be induced by temperature changes.

Procedure

The experiment was conducted during Revs 1753 through 1768. PACS was deactivated on Rev 1753 and remained deactivated until Rev 1760. After turn on the PACS performance was monitored periodically during temperature rise.

Results

Table I shows IRA and HSA temperatures when they were turned off on Rev 1753 and at the start of the thermal cycle on Rev 1760. Figure 2 is a plot of the PACS IRA Roll Gyro and IRA internal temperature monitors during warmup. Figure 3 is a plot of the PACS HSA head temperatures during warmup.

No anomalies in PACS performance were noted during this test. The previously observed IRA and HSA anomalies did not repeat leading to the conclusion that they were not temperature sensitive under the existing test conditions.

2.3 EDAP-1 through EDAP-5 - Solar Array Albedo Tests

Rationale

Future EDAP designs and contingency planning for these designs require minimum solar array output data for Lifeboat Battery life predictions with unstable vehicles. An important aspect of a potential minimum solar array

TABLE I

IRA AND HSA TEMPERATURES

Event	IRA				HSA	
	Pitch Gyro	Roll Gyro	Yaw Gyro	Internal	Left Head	Right Head
At Turn Off	167	154	159	105	85	82
At Turn On	74	69	72	69	65	68

SECRET / H

Approved for Release: 2025/06/18 C05137285

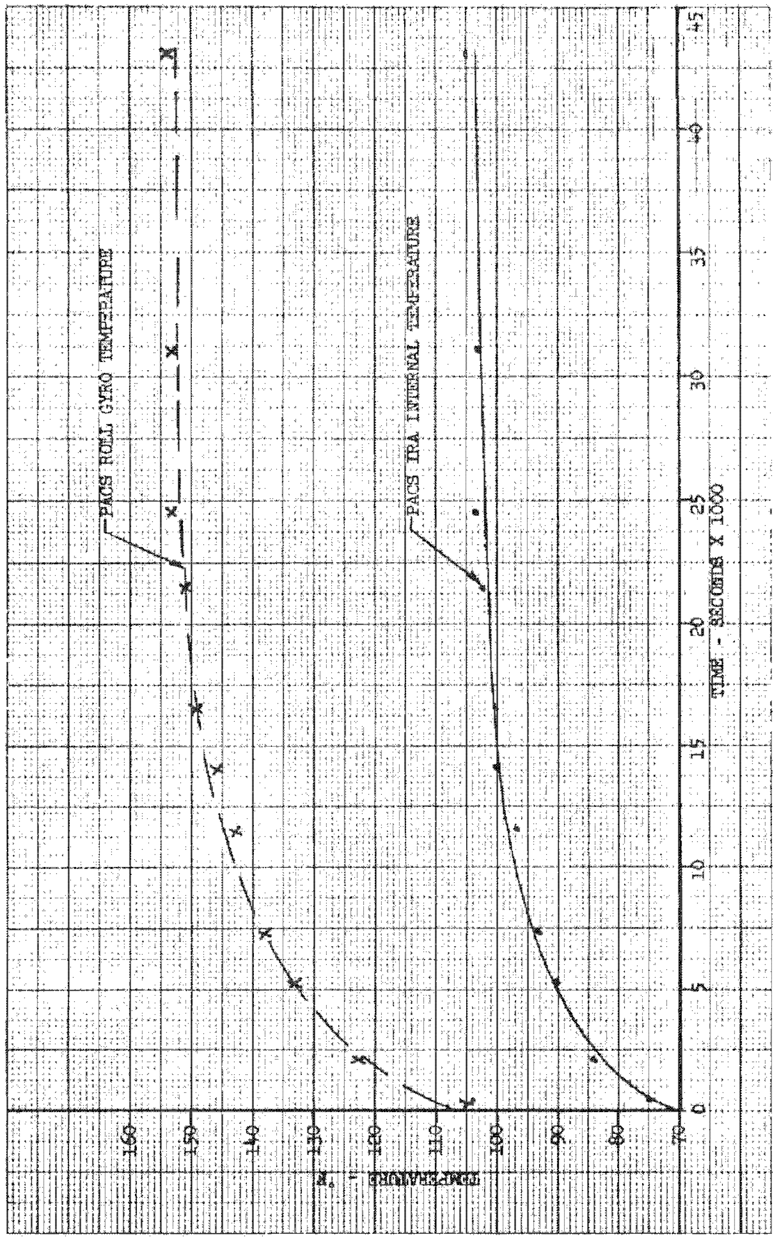

Figure 2

PACS IRA Temperature After Turn-On

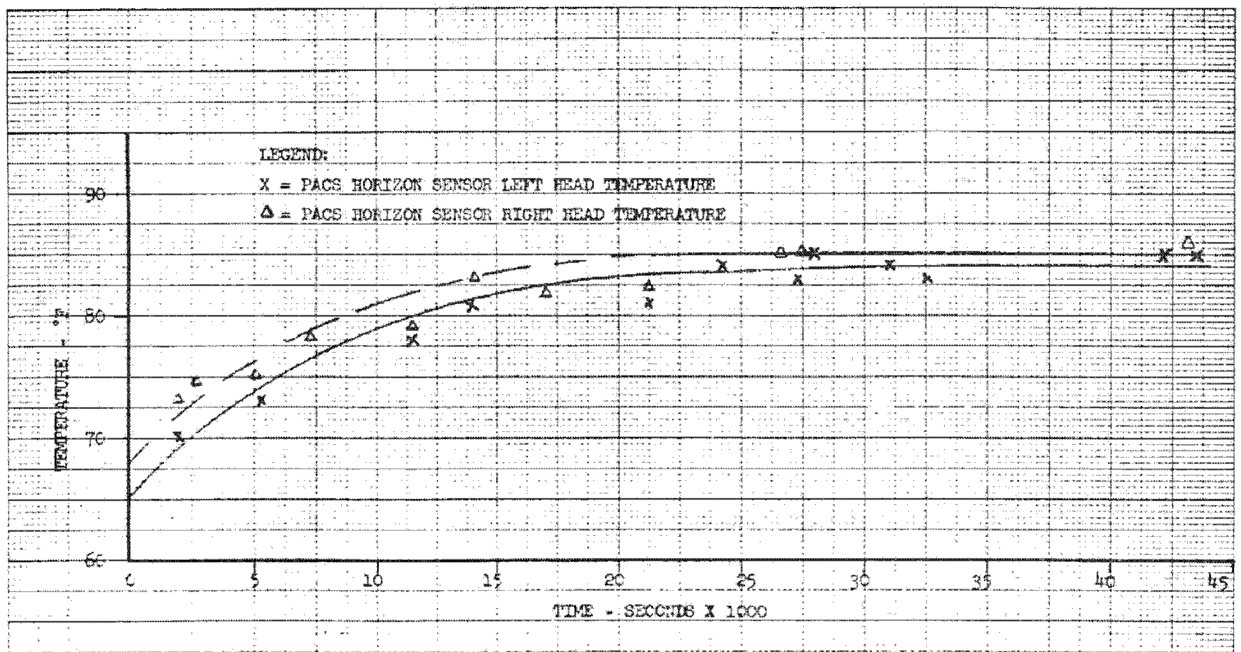

Figure 3

PACS HSA Temperatures After Turn-On

output is earth shine (albedo). The objectives of this series of tests were to determine power outputs with the arrays in various attitudes in relation to the sun and earth.

Procedure

EDAP-1: One rev of inertial flight with plane of solar array facing away from sun (perpendicular to sun rays).

EDAP-2: One rev of geocentric flight with plane of solar arrays facing toward the earth (perpendicular to albedo rays).

EDAP-3: Three revs of tumbling flight, ie, ACS/RCS disabled. NOTE: This test was cancelled.

EDAP-4: Inertial flight with plane of solar array parallel to albedo rays (end facing earth).

EDAP-5: Inertial flight with plane of solar array parallel to sun rays (end facing sun).

Results

Data on all tests were recorded continuously from exit umbra to entrance umbra. Figures 4, 5, 6 and 7 graphically depict the solar array power generation for each test configuration and Figure 8 is a comparison of the four conditions on the same time scale and starting on the exit umbra for each rev. Table II summarizes the solar array power generation in amp-hours for the test cases, a calculated tumble-mode case and a nominal output for SV-8 mission beta angle.

Solar Array Tumble Mode Calculation

Solar array data from the four EDAP tests provided power generation figures that could be integrated into values of power generation for all combinations of solar array positioning with respect to sun angle during the roll and pitch maneuvers encountered in the tumble mode. The roll rate is the primary condition required to calculate a full cycle and four revs are required to complete 360° of roll which comprised one cycle. The calculated

TABLE II

SOLAR ARRAY OUTPUTS IN AMP-HOURS FOR EDAP TESTS

TEST	ORIENTATION	* SOLAR ARRAY OUTPUT PER LEG
1	Vehicle rolled 180° in flight inertial orbit. Solar Array looking at earth albedo.	1.17 amp-hours per rev
2	Vehicle rolled 180°. Geocentric orbit. Solar Array facing local horizontal on the earth.	1.76 amp-hours per rev
3	Vehicle tumble mode	1.46 amp-hours (calculated)
4	Vehicle rolled 90°. Sun angle 26°. Inertial flight with Solar Array looking into space and edge pointed toward earth.	0.51 amp-hours per rev
5	Vehicle rolled 90° plus sun angle. Inertial Flight with Solar Array looking into space with edge pointed toward sun.	0.33 amp-hours per rev

* Normal output of Solar Array in normal vehicle orientation = 5.90 amp-hours per rev.

Approved for Release: 2025/06/18 C05137285

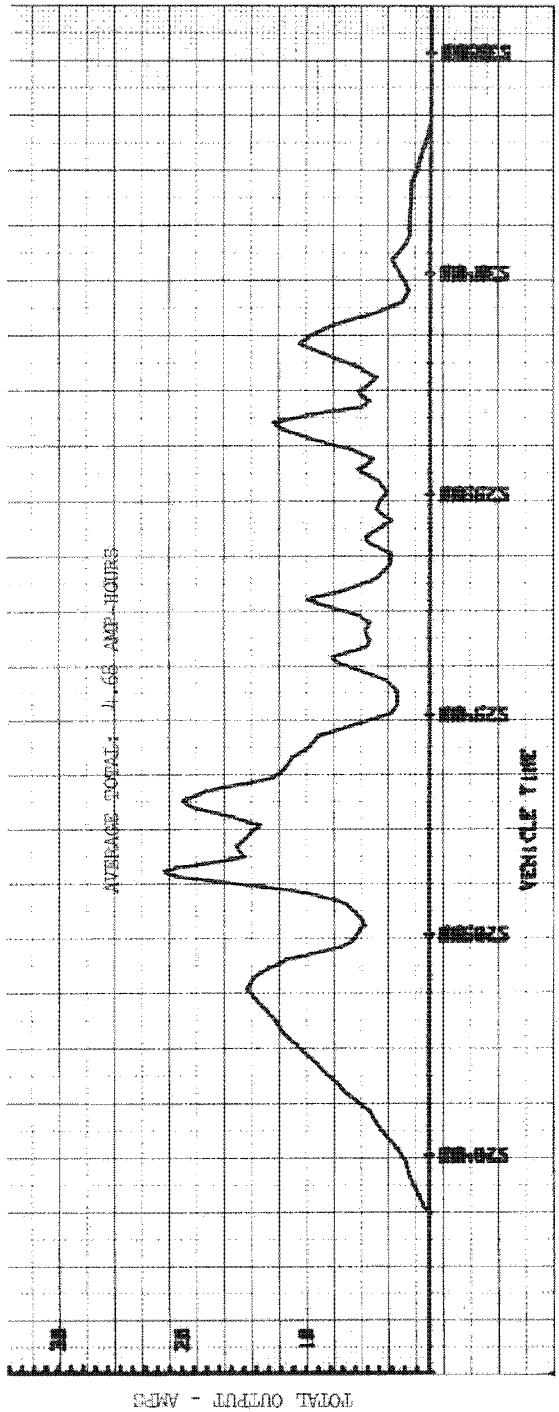

Figure 4
Solar Array Output for Rev 1200, EDAP 1 Test

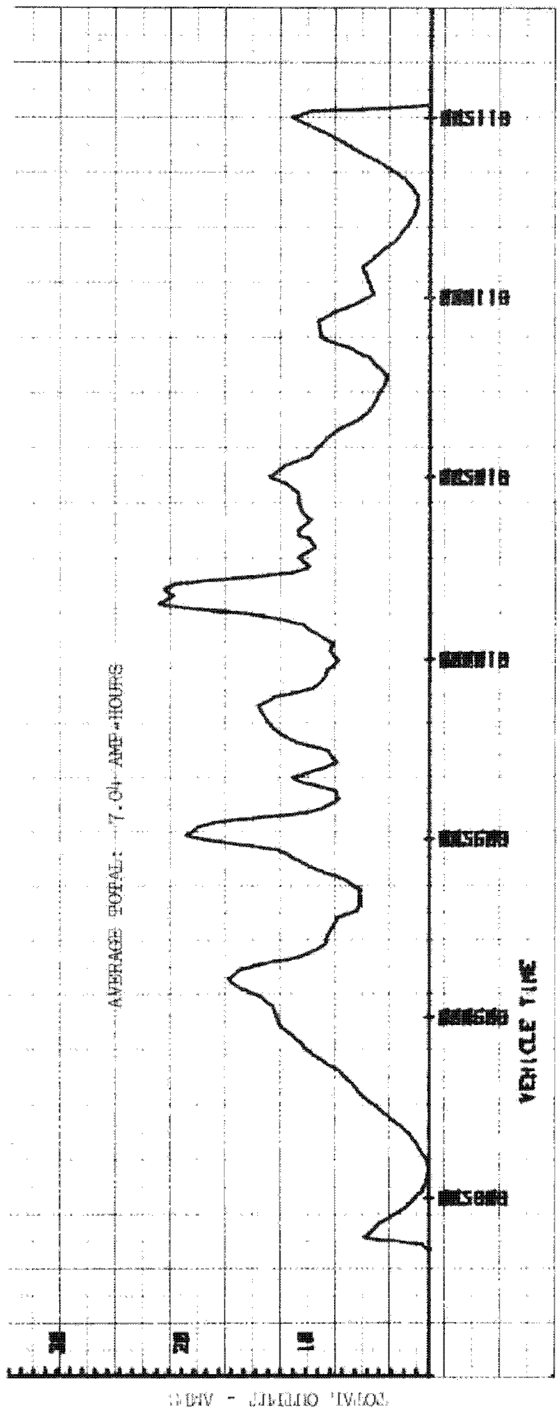

Figure 5
Solar Array Output for Rev 1725, EDAP 2 Test

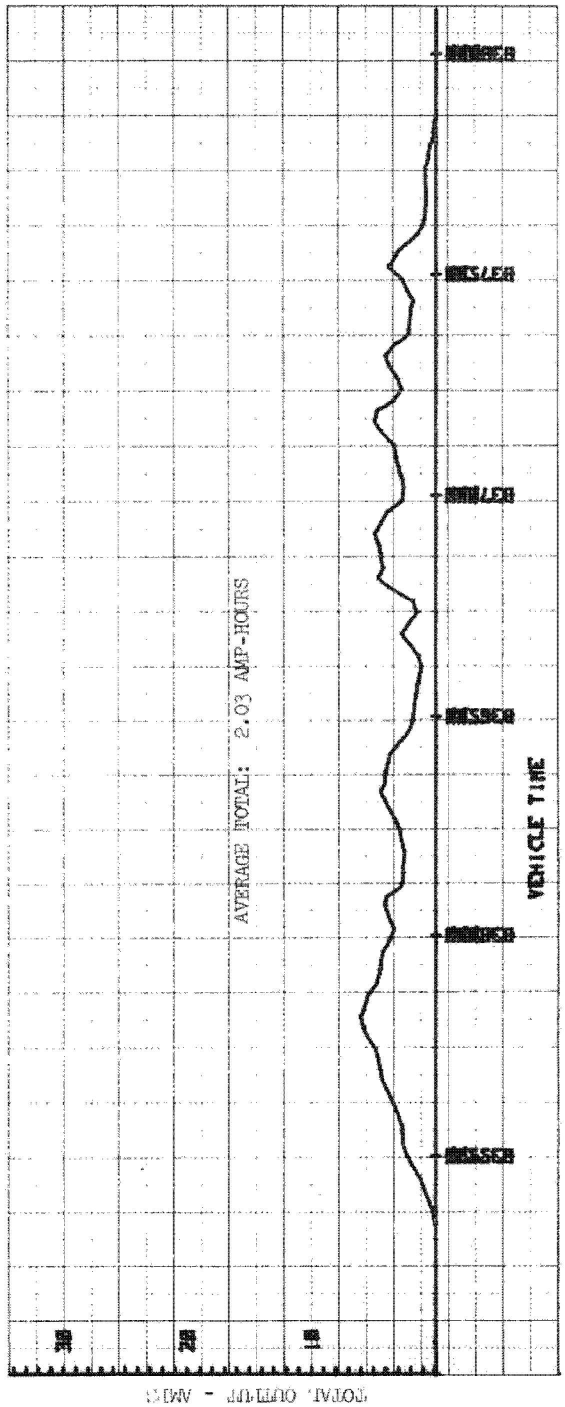

Figure 6
Solar Array Output for Rev 1730, EDAP 4 Test

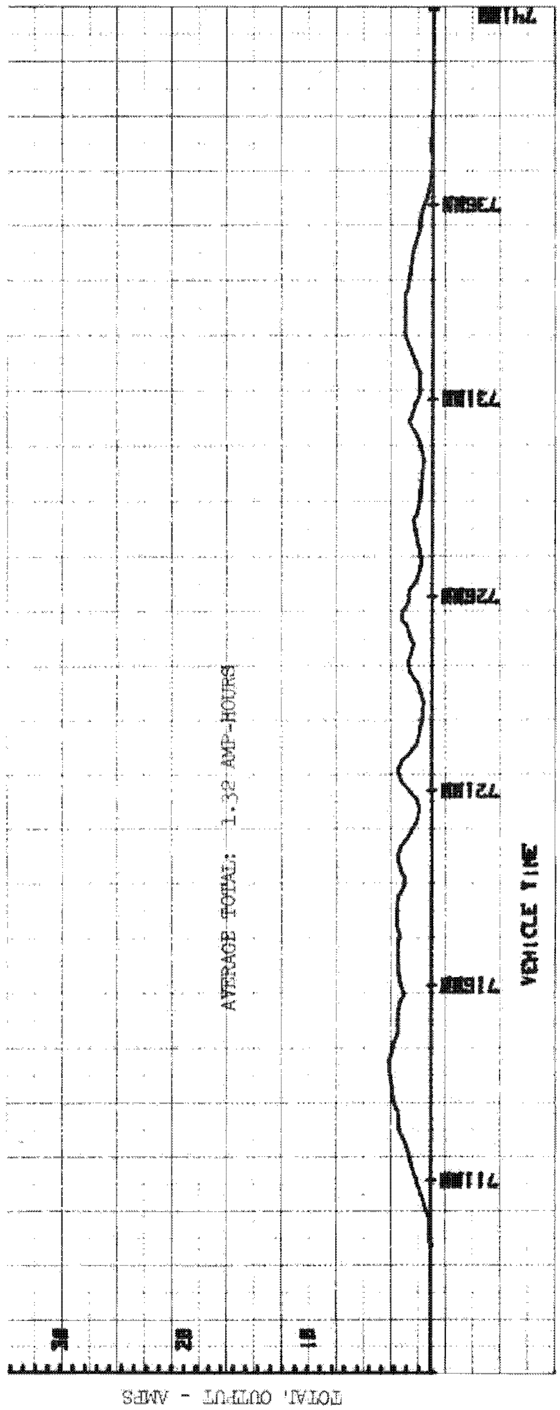

Figure 7
Solar Array Output for Rev 1744, EDAP 5 Test

SECRET / H

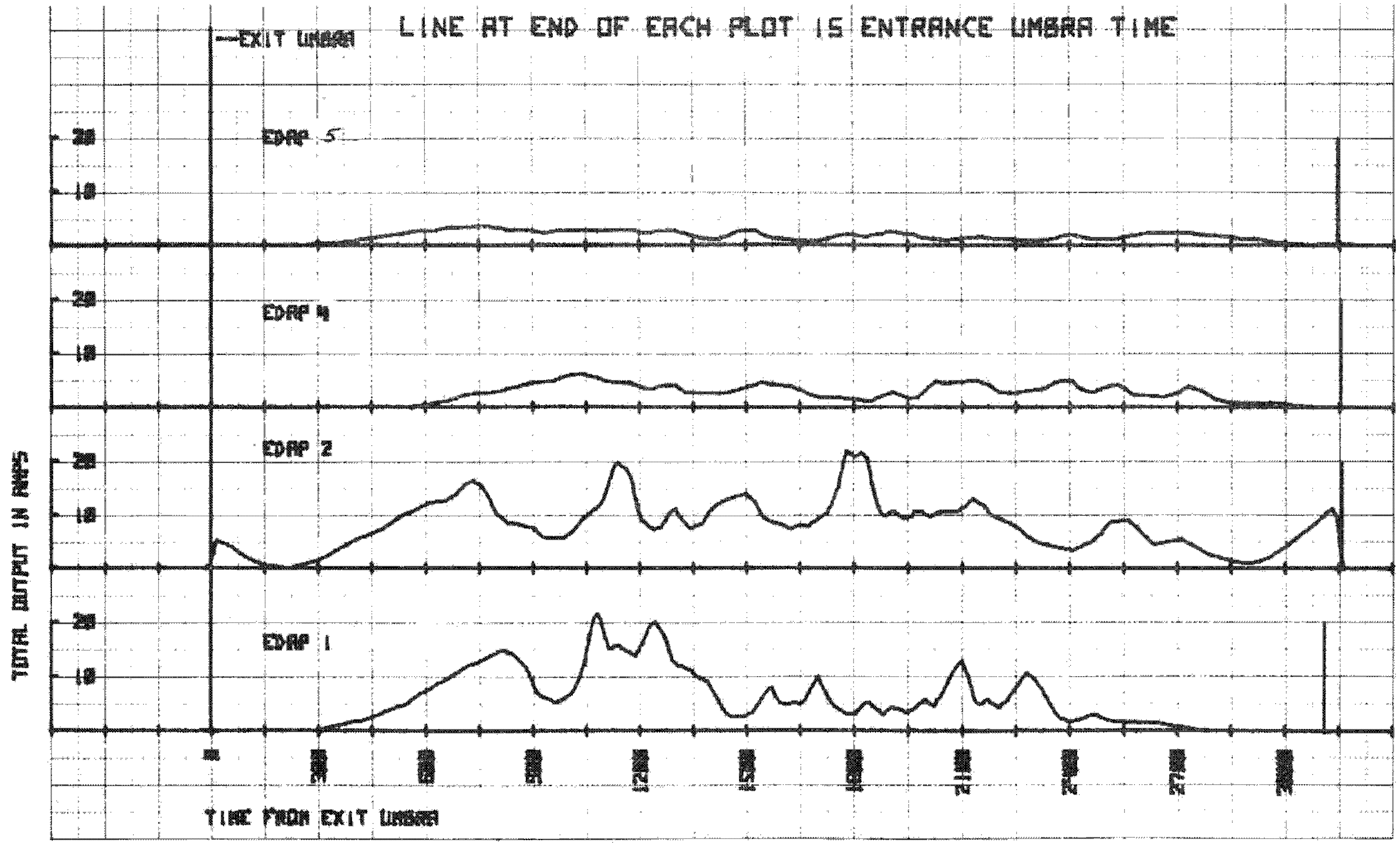

Figure 8

Comparison of EDAP Test Outputs on Same Time Scale and Same Reference Point (Exit Umbra)

SECRET / H

BIF003W/2-091480-74

Approved for Release: 2025/06/18 C05137285

values for power generated during a tumble mode over four complete revolutions averaged 1.46 amp-hours/rev. Other combinations of pitch and roll rates could be used for calculating power generation but any combination would eventually attain a complete cycle which would result in an amp-hour average/rev approximately equal to these calculations.

2.4 OAS-1, OAS Propellant Mass Status

Rationale

The purpose of the OAS Solo experiment was to obtain data regarding the accuracy of OAS Tank propellant mass determinations. Techniques currently used are (1) the integration of propellant flow rate through the Thrust Chamber Assembly (TCA) venturi, and (2) the calculation of OAS gas ullage volume growth. During the course of the mission an ever increasing bias between these two methods was observed.

Procedure

The OAS propellant tank depletion point was determined by observing the loss of engine (TCA) thrust through propellant depletion. After completing a 230.8 second deboost firing (OA 45) on Rev 1768 and coasting for 11.6 minutes, a 270.0 second TCA firing was programmed to consume expected propellant residuals plus 50 pounds. The TCA firing was scheduled to acquire OAS performance data in real time over the last station pass.

Results

Analysis of test data showed that the TCA venturi method of estimating OAS propellant mass status provides values well within requirements but inaccuracies in the gas law determination method were larger than anticipated. Based on integration of TCA venturi flow rates and an estimate of RCS propellant consumption (from the OAS Tank) in the period between Revs 938 and 1083, the tank depletion point was expected to occur 185 seconds into the tank depletion firing (OA 46). The expected rapid drop in TCA chamber pressure and Catalyst Bed pressure actually occurred at approximately 195 seconds as shown in Figure 9 (with about 4 pounds of propellant remaining in the tank at this time).

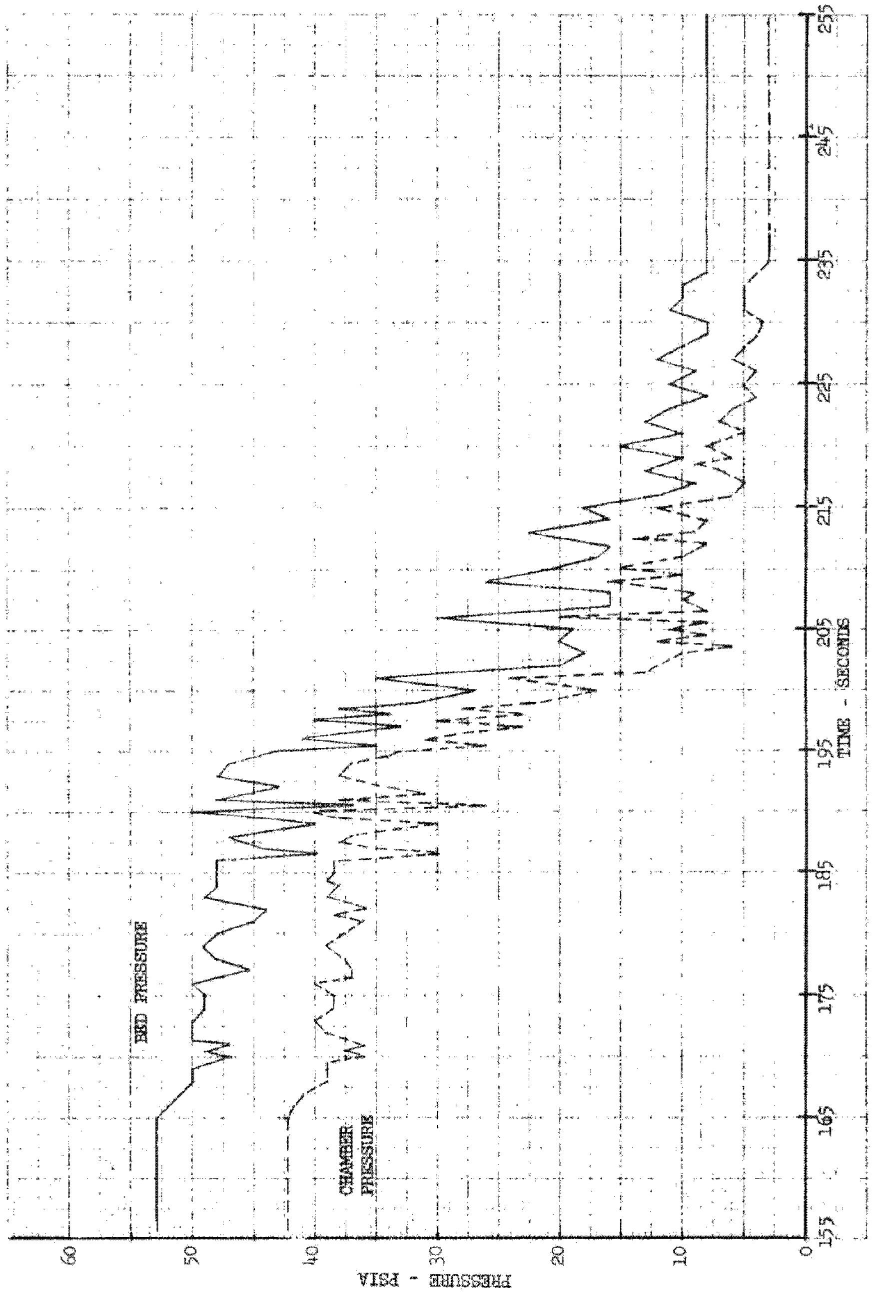

Figure 9
Orbit Adjust 46, Propellant Depletion Run

Gas injection into the engine began unexpectedly early at 165 seconds into the firing and continued throughout the depletion process.

As stated above, determination of the propellant depletion time made possible an evaluation of the accuracy of both the venturi and gas law mass status techniques. The venturi method was shown to be very accurate, differing from the actual value by only 2.3 lbm at deboost. However, the gas law method was shown to be in error by 143 lbm (versus ±100 lbm allocated). A number of mechanisms are being investigated in an effort to explain the mass status errors, including propellant loading variations, tank volume errors, nitrogen solubility, gas evolution, pressure transducer shifts, and data processing.

At present it can be concluded that the accuracy of the venturi mass status technique is within expected limits while the gas law technique is not as reliable and exhibits errors greater than expected from analysis. Therefore, the venturi method will be used for OAS propellant mass status operationally to the greatest extent possible.

TCA Summary

The engine performance was normal for both the active and Solo phases of the mission. The values for propellant thruput (3189 lbm) and total impulse (745,000 lbf-sec) were the largest attained to date.

2.5 RCS-1, RCS 1 Storage Effects

Rationale

The purpose of this test was to evaluate the effect of a long storage period on RCS 1 System.

Procedure

On Rev 1082 the Primary RCS System was turned off due to low thrust on REA's 1, 8 and 7 and reactivated during the Solo portion of the mission, Rev 1741. SV-7 had a similar set of conditions when the primary system was shut down on Rev 1446 and reactivated on Rev 1768.

Results

A comparison chart, Table III, is presented for the two vehicles showing the normalized thrust just prior to shut down and the thrust shortly after the system was reactivated. Table III shows that in every case an extended storage period has an adverse effect on a thruster that was degraded at the beginning of the storage period while the nominally performing thrusters remained essentially the same.

Changes to the REA Catalyst Bed, both physically and chemically, could have occurred during the storage period such as:

(1) Change in feed pressure

(2) Physical change to injector and/or bed.

(3) Altered chemical activity of the bed

Based on the tabulated data two conclusions can be drawn:

(1) If the REA thrust level is nominal prior to the storage period it will perform nominally after the storage period.

Consider XFER TO SIDE 2 PRIOR TO DEGRADATION

(2) If the thruster performance level is degraded prior to the storage period it may reactivate at its former level but most likely will have suffered additional degradation up to 50% of the original level.

2.6 THERM-1, Sun Exposure Experiment

Rationale

This experiment was designed to expose the six vehicle axes to the sun for a period of 30 minutes to assess potential thermal impact as a result of vehicle maneuvers and to develop operational constraints if test results warranted .

NOTE: This experiment was not performed due to lack of Solo time and its relatively low priority rating.

TABLE III

SV-7 AND SV-8 RCS THRUST LEVELS

Rev	THRUSTER							
	1	2	3	4	5	6	7	8
SV-8								
1082	3.14	*5.02	1.62	*4.61	*5.06	*4.91	2.89	1.17
1741	2.07	*4.91	0.76	*4.58	*4.91	*4.69	1.42	0.87
SV-7								
1411		4.00	*5.20	3.00	2.60	3.15	*5.32	3.20
1768		2.05			1.89			
1801			*5.01	2.13			*5.13	
1816								1.94
1833						2.16		

*Indicates thruster was not degraded at the time the primary system was turned off.

2.7 THERM-2, Simulate -30° Beta Angle

Rationale

The purpose of this experiment was to assess the ability of the battery bays to maintain an operable environment at a -30° Beta angle; to assess Aft Section contamination on +Y surfaces and, to demonstrate the symmetry in the thermal design of the Mid and Forward Sections.

Procedure

Flying in a reverse attitude effectively puts the vehicle in a -30° Beta angle position. The fly reverse was performed on Rev 1753 and continued through deboost, Rev 1768 (15 revs). The effective resultant Beta angle was -28°.

Results

Aft Section

This experiment confirmed that with the exception of the battery bays, the new Aft Section thermal design was capable of maintaining acceptable temperature environment for all bays. The thermal performance of the Aft Section in this attitude was compared to preflight predictions for Beta = -30 degrees with normal forward attitude. Equipment Section door temperatures and Reaction Control Section (RCS) skin temperatures correlated well with preflight predictions. The aft bulkhead was 25 to 35 degrees above the predictions which may be attributed to aerodynamic heating on the bulkhead. In turn, the warmer bulkhead resulted in RCS plumbing and tank temperatures 10 to 15 degrees above predicted values. Most Equipment Section boxes reached stable temperatures during this test and all equipment remained well within limits throughout the experiment. Table IV compares critical equipment temperatures with design limits.

The battery bay door temperatures stabilized within the predicted range; however, battery temperatures went above heater control limits early in the test, continued to rise and at the conclusion of the test all batteries were in the 48 to 59° region. Since battery heat dissipation increases with temperature, it was not possible to predict a stabilized range

Should probably keep the -8° Beta Constraint.

TABLE IV

AFT SECTION CRITICAL COMPONENT TEMPERATURES

CRITICAL COMPONENT	DESIGN LIMITS (°F)	SV-8 ACTUALS (°F)
PDJB	-30/165	100/102
CCC 2	-30/170	113/114
Type 25 Batteries, Bay 3	35/70	52/54
Type 30 Battery	30/90	53
Type 31 Batteries	40/90	52/54
Type 29 Batteries, Bay 4	35/70	48/50
HSA Heads	0/130	82/87
IRA's	50/130	104/114
PCM Master	-30/170	87/102
Tape Recorders	20/120	84/93
Transmitters	-30/170	80/102
ECS Clocks	40/153	92/95
ECS PMU A	-40/145	81/82
ECS PMU B	-40/145	89/90
IRA Gyro	50/200	151/171
MCS	-40/149	61
RCS Tanks	40/140	85/101
Plumbing, Bay 6	35/140	90/97
Plumbing, Bay 12	35/140	90/107
OA Tank	70/100	89/91
PDA's	-30/160	87/113
Solar Arrays	-125/225	-65/145
Quad Valve	40/200	132/134

for the batteries. A longer "fly reverse" experiment, perhaps of 5 days duration, would be needed to define battery thermal performance.

Mid-Forward Section, APSA

In the Mid Section, Forward Section, and APSA the thermal designs are symmetrical, and therefore it could be expected that given enough time to achieve equilibrium, the fly reverse experiment would cause temperatures to reverse. During THERM-2 recorded temperature data was obtained after nine revs of reverse flight and again after fourteen revs, and the indications were that equilibrium had been reached.

It was found that in all cases the symmetrical design resulted in temperatures as predicted and that temperatures were reversed as expected. In the case of the Forward Section and APSA, there was a small overall decrease in temperature which is believed to be due to the absence of free molecular heating. This temperature decrease amounted to about 3°F in the Forward Section Bay 4 and about 6°F in T_{ENC}, the average APSA structure temperature. It is believed that the change in APSA temperature would be less with the Recovery Vehicle still aboard.

2.8 TT & C-1, SGLS 1 Non-Coherent Frequency Measurement

Rationale

The General Dynamics Electronics Transponder used in the SGLS 1 position had exhibited a drift trend in its crystal controlled non-coherent frequency during vehicle ground testing. The drift trend was believed to be caused by aging of the crystal. If the trend continued at its existing drift rate, it was predicted that the non-coherent frequency would be outside the specification limits of ±68 KHz of nominal center frequency (2277.5 MHz) before the end of the SV-8 mission. Because of RTS capability, however, this condition would not present an operational problem.

The transponder worked well throughout the active mission and it was desirable to determine to what extent the drift trend had continued by making a measurement of the non-coherent frequency during the Solo phase, for engineering information.

Procedure

The measurement was made at station pass 1757 Cook at acquisition, mid pass, and fade. The actual measurements made gave the following frequencies:

Acquisition:	2277.50 MHz
Mid Pass:	2277.46 MHz
Fade:	2277.40 MHz

The last recorded ground test reading of the non-coherent frequency, taken about 6 days before launch was -57.4 Kz from nominal (an average of two readings). The flight data at mid pass therefore indicates that the frequency drift did not degrade during the mission, within the resolution of the RTS frequency measurement capability.

2.9 TT & C-2, PCM Remote Unit 4A Diagnostic Test

Rationale

During the mission PCM Remote Unit 4A failed to reply to a Master Unit data request commencing at the start of a record sequence on Rev 1023. Subsequent testing and analysis narrowed the failure mode to approximately 9 modules within the Remote Unit. The purpose of this test was to operate RU 4A with PCM Master Unit 2. This configuration uses a different Remote Unit party line interface than the normal PCM MU 1/RU 4A interface and could have narrowed the failure mode down to two RU modules if the test were successful.

Procedure

The special diagnostic test was conducted on Rev 1710 operating RU 4 with PCM MU 2.

Results

The RU 4A still failed to reply to Master Unit 2 data requests, and the number of RU Modules possibly involved in the failure mode was not reduced.

2.10 OPS-1, Redundant Systems Performance

Rationale

OPS-1 consisted of a total of 12 tests (a) through (l) with the object of evaluating redundant systems performance. A brief description of each test and a brief summary of results are presented here.

OPS-1(a) - SGLS 2

Results: SGLS 2 output power dropped 20 dB during the primary mission - probably caused by a loss of pressure in the RF cavity output stage. If SGLS 2 had been required to support operations, data reception might have been adversely affected with RTS having only the 14 foot antenna.

ha! practically unusable

OPS-1(b) - MCS, PCM 2B, TPS2, APS2, FPS2

Results: MCS functional health was verified in Segment One and again on Rev 1765 POGO. PCM 2B, TPS2, APS2, and FPS2 activations were also successfully demonstrated on 1765 POGO.

OPS-1(c) - Aft Switched Bus to Lifeboat Battery

This test was eliminated due to other test restrictions during Solo.

OPS-1(d) - Backup Timer

Results: The Backup Timer Test was performed on Rev 1466 HULA with a successful time out that was in agreement with the R-1 day time out.

OPS-1(e) - Lifeboat Execute

Results: This test was part of Q-21 and was successful.

OPS-1(f, g, h, i) - Verification of Redundant Heaters

Results: On Revs 1734 and 1735 the operational status of the OAS and RCS Redundant Heaters was verified.

OPS-1 (j) - Redundant TCEA Test

Results: The Redundant TCEA was activated on Rev 1669P and operated for 16 revs. Performance was nominal.

OPS-1 (k, l) - DBS Redundant Heaters and Oscillator

Results: DBS Redundant Systems operated successfully on Revs 1004 through 1053.

OPS-1 (m) - SCC 2 Health Test

Results: The SCC 2 Health Test was performed on Rev 966 during the primary mission and was successful.

2.11 OPS-2 - SV Life Capability

Rationale

Assess the ability of the SBA station keeping subsystems to sustain undegraded vehicle performance for extended missions.

Procedure

Use primary and redundant systems as necessary to support primary mission requirements for as long as possible including the Solo Phase.

Results

The primary mission terminated with recovery of RV 4 on Day 106 and the flight terminated with deboost on Day 110 due to propellant depletion.

ACS-1 roll gyro rate output became noisy on Rev 1479. Although no vehicle response resulted from the noise signal, transfer was made to ACS-2 on Rev 1501. After the transfer the noise signal disappeared. (Reference Solo Experiment ACS-2). ACS-1 Horizon Sensor pitch and roll output showed deviations from normal starting on Rev 1586. These deviations continued intermittently at random during the remainder of the mission (ACS-1 not controlling). RCS-1 was used from lift-off until Rev 1083 (Day 67). At that time RCS-1 capability had become marginal and control was transferred to RCS-2 for the remainder of flight, except for specific RCS Solo Tests.

The orbit was maintained with orbit adjusts at 3-day intervals throughout the mission.

Electrical power was available for all programmed mission activity. No power usage constraints were required in support of primary and secondary payloads however, a Quantic power limitation was imposed in Segment One as a precaution against excessive battery depletion.

TT & C subsystem evidenced two anomalous conditions neither of which had an adverse effect on mission objectives. On Rev 1023 PCM Remote Unit 4A failed but operations were successfully continued by switching to Remote Unit 4B. A SGLS 2 Health Test on Rev 1426 Hula showed the transmitter power output to have decreased by 20 dB probably caused by a loss of pressure in the RF cavity output stage with resultant corona. Subsequent testing indicated that receipt of data might possibly have been adversely affected with RTS having only the 14 foot antenna.

2.12 Q-1 through Q-25 Quantic Experiment

For convenient reference acronyms used in this section that are peculiar to the Quantic Experiment are listed.

CEU	Central Electronics Unit
DG MAP	Predicted Magnetic Map
HSS	Horizon Sensor System - Either Barnes or Quantic
HT	Horizon Tracker - Individual Sensing Head
LB II	Lifeboat
PDWN	STC Mode Pitch Down Indicator
OA+	Positive Orbit Adjust
OA-	Negative Orbit Adjust
Q	Quantic
QI	Quantic Industries - Contractor for the HSS and STS
RV	Recovery Vehicle
STS	Star Tracker System
ST	Star Tracker - Individual Sensing Head

Introduction

The Quantic Industries (QI) experiment consisted of a complete Star Tracking System (STS) and Horizon Sensor System (HSS) and was flown in a piggy-back non-controlling configuration on SV-8. The integration of the experiment equipment with the SV, the pre-flight testing, the operational support required and finally, the in-flight and post flight data reduction and analysis effort all represents substantial commitment on the part of many organizations. A comprehensive and detailed report of these activities is beyond the scope of this document and will be reported on separately at a later date.

However, since Quantic testing represented the major portion of Solo testing on SV-8, very brief summaries of the 25 sub-experiments are listed here to provide a complete record of the Solo Phase. In some instances (Q10, Q19, Q21 and Q24) the resultant test data has been expanded because it is available.

Experiment Description

The experiment consisted of both a Quantic Industries Horizon Sensing and Star Tracking Subsystems. The Horizon Sensing System consisted of four independent Horizon Trackers (H/T) and a Central Electronics Unit (CEU) which processed the H/T angle outputs to form pitch and roll attitude estimates. The Horizon Sensor CEU also performed the telemetry subcommutation and power supply functions. Two independent Star Trackers and an additional CEU formed the Star Tracking System.

Because of the selected geometry for mounting the experiment trackers to the vehicle, it was not possible to mount all trackers on the same integral structure. As a result, the configuration shown in Figure 10 was flown. Both Star Trackers and three Horizon Trackers were mounted on a large pylon located at Bay 8 on the aft bulkhead of the Aft Section. One H/T, which looked forward and down was located on the aft bulkhead of the Aft Section at Bay 5. Since pitch and roll attitude could be extracted from any three of the four HTs as well as the two (both required) single axis S/T, the large pylon configuration was sufficient to compare the QI attitude sensing system with the Barnes H/S System.

Quantic Test Profile

Date	Rev	Test
April 12	29	Q-1
April 15	81.9	Q-1 (ST)
April 16	94	Q-9 (OA+)
April 16	95	Q-8 (Yaw Reverse)
April 16	96	Q-9 (OA-)
April 16	96	Q-8 (Yaw Forward)
April 17	113	Q Calibrate
April 17	114	Q-13
April 17	114	Q-13 ST+
April 17	115	Q-13
April 17	115	Q Calibrate

Date	Rev	Test
April 18	130	Q Calibrate
April 18	131	Q-13
April 18	132	Q-13
April 18	135	Q-11
April 19	143	Q-9 (OA+)
April 19	146	Q-3
April 19	150.3	H/T-
April 20	162.8	Q-3
April 21	178.8	Q-3
April 22	192	Q-9 (OA+)
April 22	195.0	Q-3
April 22	195.3	Q H/T+
April 24	228	Q-7
April 25	240	Q-9 (OA+)
April 25	241	Q-8 (Yaw Reverse)
April 25	242	Q-9 (OA-)
April 25	242	Q-8 (Yaw Forward)
April 26	260	Q-4A
April 26	261	Q-4B
April 27	271	Q-5A
April 27	272	Q-5B
April 28	289	Q-9 (OA+)
April 28	292	Q-13
April 29	308 - 310	Q-11
May 1	337	Q-9
May 3	375.8	Q-4A
May 3	376.8	Q-4B
May 4	326.6	Q-9 (OA+)
May 4	387	Q-8 (Yaw Reverse)
May 4	388	Q-9 (OA-)
May 4	388	Q-8 (Yaw Forward)

Date	Rev	Test
May 5	406/7	Q-13
May 7	434	Q-9 (OA+)
May 8	453	ST 1 Failure
May 8	455	Q Power Down
May 8	465	Q Power Up
May 10	483.2	Q-9 (OA+)
May 11	489.7	Q-4
May 11	490.7	Q-4
May 12	518	Q-13
May 12	519	Q-13
May 13	532	Q-9 (OA+)
May 13	533	Q-8 Yaw Reverse)
May 13		Q-9 (OA-)
May 13		Q-8 (Yaw Forward)
May 15	580.4	Q-9 (OA+)
May 17	602.8	Q-4
May 17	603.8	Q-4
May 19	615/17	Q-13
May 19	629.4	Q-9 (OA+)
May 22	681	Q-7
May 23	683	Q-9 (OA+)
May 24	714	Q-4A
May 24	716	Q-4B
May 25	726.6	Q-9 (OA+)
May 25		Q-8 (Yaw Reverse)
May 25		Q-9/Q-8 (Forward)
May 26	741/2	Q-13
May 28	774.2	Q-9 (OA+)
May 30	811.8	Q-4A
May 30	813.7	Q-4B
May 31	823.4	Q-9 (OA+)

Date	Rev	Test
June 3	871	Q-9 (OA+)
June 3	887/88	Q-13
June 5	920	Q-9 (OA+)
June 5	921	Q-8 (Yaw Reverse)
June 5	922	Q-9 (Forward)
June 9	965	FA Cal
June 9	972	Q-8 (Yaw Reverse)
June 9	973	Q-7
June 9	973	Q-8 (Forward)
June 10	975	Q-9 (OA+)
June 10	984/985	Q-13
June 12	1017	Q-9 (OA+)
June 12	1021/1022	Q-11
June 15	1066	Q-9 (OA+)
June 16	1082	Q-8 (Mini)
June 16	1084	Q-7 (Pitch Down Test)
June 17	1093	Q-Cal
June 17	1099	Q-7, Q-8
June 17	1099	All Off
June 18	1108	Q-ON
June 18	1118	Q-7 (Man)
June 18	1120	Q-9 (OA+)
June 19	1130	Q-7/Q-8
June 19	1130	All Off
June 19	1139	Q-ON
June 21	1162/1164	Q-9 (OA-)
June 21	1166/1167	Q-4
June 22	1178/1179	Q-13
June 23	1199/1200	Q-10
June 23		Q-Off

Date	Rev	Test
June 24	1211	Q-On, Q-9 (OA+)
June 24	1218	Q-7, Q-8
June 24	1218	Q-Off
June 25	1227	Q-On
June 26	1248	Q-20A
June 26	1260	Q-9 (OA+)
June 27	1264	Q-4
June 28	1283	Q-9 (OA+)
June 28	1283	Q-20A
June 29	1295	Q-20A
June 30	1314	Q-9 (OA+)
July 1	1329	Q-20A
July 3	1357	Q-9 (OA+)
July 3	1362	Q-20A
July 4	1376/1377	Q-11
July 5	1392/1394	Q-4
July 6	1406/1408	Q-9 (OA-)
July 6	1409	Q-20A
July 7	1420/1421	Q-13
July 7	1425	Q-20A
July 9	1457/1459	Q-4
July 10	1470	Q-2
July 10	1473/1474	Q-11
July 11	1490	Q-20A
July 12	1501	M1V2/M2V2
July 12	1502	Q-9 (OA+)
July 15	1551	Q-9 (OA+)
July 15	1555.1	Q-2
July 18	1600	Q-9 (OA+)
July 19	1616	Q-9 (OA+)
July 19	1619/1621	Q-4

Date	Rev	Test
July 20	1632	Q-16
July 20	1635/1637	Q-11
July 21	1669/1670	Q-13
July 22	1701	Q-7
July 24	1704	Q-9 (OA+)
July 24	1704	Q-22
July 25	1705	Q-16
July 25	1707	Q-13(F)
July 25	1714	Q-17
July 25	1715	Q-13 (A)
July 25	1715	Q-11(A)
July 25	1716	Q-13(A)
July 25	1718	Q-20B
July 26	1720/1723	Q-10B
July 26	1723/1735	Q-24
July 26	1738/1739	Q-17A
July 27	1747	Q-23
July 27	1750	Q-25
July 27	1751	Q-21
July 27	1753/1760	ACS-2
July 27	1753	Q-8
July 28	1753	Q-8
July 28	1756/	Q-11
July 28	1757	ACS-1
July 28	1763/1765	Q-18
July 28	1765	ST A+

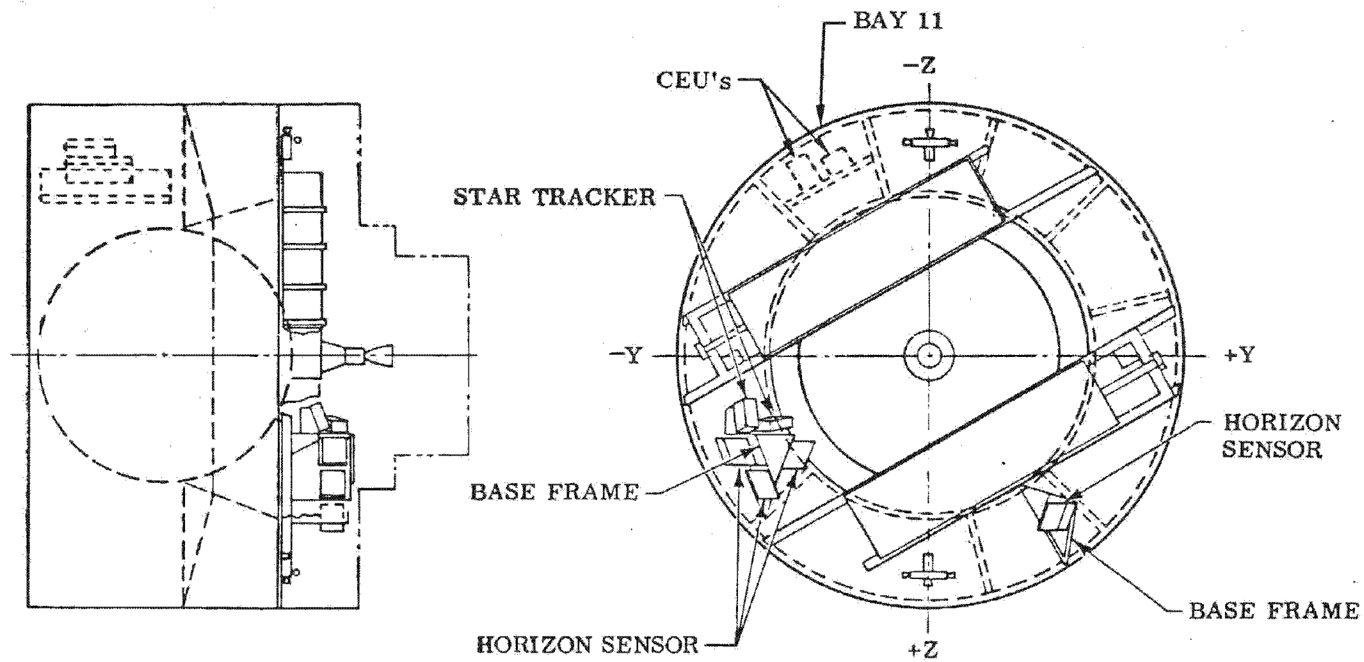

Figure 10

Quantic Experiment Integrated Configuration

Objectives

The primary objectives of the experiment are listed below:

1. Construct an experiment to approach a true flight configuration for both horizon sensing and star sensing attitude measurement systems.
2. Use the combination of experiment sensors to determine accuracy of the Quantic horizon sensing and star tracking systems as well as the Barnes horizon sensing systems.
3. Test the equipment in flight to ascertain if critical specifications are being met.
4. Provide the interfacing experience for the Quantic Horizon Sensor.
5. Perform a meaningful experiment to gather information about the effect of horizon radiance noise on both the Quantic and Barnes Horizon Sensors.

In addition the following secondary objectives were persued:

1. Provide the data by which present (or future) attitude estimation schemes can be judged.
2. Provide flight experience in gathering data for ground processed attitude estimation.
3. Provide an accurate test of gyro drift on pitch and roll axes.
4. Provide an accurate test of maneuvering on pitch and roll axes.
5. Provide flight test information on H/S inhibit attitudes.
6. Evaluate S/T performance in daylight.

Q-1 Quantic Evaluation Health Test

Objective

An initial status check on the star sensing and horizon sensing systems during flight conditions and to determine the accuracy of each of the on-board sensors with respect to the others.

Results

This experiment was performed on Rev 29 and again on Revs 81/82. The following information was obtained:

- Star Tracker sensitivity was higher than anticipated (visual magnitude 5 rather than visual magnitude 3).
- An offset shift was observed between the small pylon HT head and the three large pylon HT heads.
- QI equipment temperatures on the aft bulkhead (temperature sensors located on the HT heads) were 15 to 20°F lower than predicted. Later in the mission temperatures dropped further to 30 to 40°F below predicted values. These temperatures were within specification limits and there was no indication that system performance was affected.

Q-2 Pitch (Alpha) Bias Check

Objective

To check successful application and removal of the pitch bias.

Results

This experiment conducted on Revs 1470 and 1555. The application and removal of the pitch bias to the pitch analog channel was successful. Also the "fast lock-on" capability (2°/second) of the individual horizon tracker was verified.

Q-3 Star Catalog Check

Objective

Perform an update of the flight star catalog to be used for downstream experiment planning. Also, the S/T calibration curves for angle corrections as a function of silicon magnitudes will be checked.

Results

Conducted daily early in the mission and twice daily in the latter part of the mission. The observation resulted in identifying (to date) approximately 150 stars some of which had visual magnitudes as dim as magnitude 5. Based on these findings it has been estimated that the flight star tracker sensitivity would result in a catalog of about 1500 stars for this specific experiment. It was originally predicted that the tracker sensitivity would result in a 100 star catalog (first hundred brightness stars).

Q-4 Weekly (H/S) Drift Calibration Check/Star Catalog Check

Objective

Detect and measure any drift or shift in the QI H/S output since the last calibration, which includes short term drift (1 to 2 rev span) and long term drift (1 week). Also, a continuing check on star availability for downstream experiment planning will be derived from this data.

Results

This sub-experiment was conducted at approximately weekly intervals. Data indicated that drift characteristics of the horizon trackers were sufficiently small that calibrations would not be required at weekly intervals. In fact, no drift was observed when calibrations were scheduled at two week intervals.

Q-5 Sun Signature (Nose Forward/Nose Aft)

Objective

Assess sun interference problems associated with the QI Star Trackers operating in the daylight portion of the rev.

Results

Early data indicated unsatisfactory performance by the star trackers in the daylight portion of the rev. This had been predicted because no sunshades had been included in the protective covering design. Limited performance was obtained for the first few hundred seconds of orbital sunrise. This could possibly be explained by aft bulkhead shading when vehicle is in the nose forward attitude.

Q-6 Health Checks

Objective

Analyze flight behavior of the experiment on a continuing basis throughout the mission.

Results

Status data were collected on each rev. Health checks were a valuable source of experiment status, eg:

- Equipment temperatures were found to be substantially lower than predicted throughout the flight.
- Drift calibration sequences were modified due to horizon tracker hangup that was observed during a health check.
- Star Tracker 1 failure was observed on a health check on Rev 454.

Q-7 Pitch Maneuvers

Objective

Determine characteristics of Quantic H/S when operating at a pitch offset. During large pitch maneuvers, the QI H/S will inhibit. The characteristics of the inhibit will be obtained for future analysis related to the geometry of inhibit conditions. The capability of the Horizon Trackers to track the horizon at significant pitch rates and abnormal pitch angles will also be checked. If stars are available during the maneuvers a check on maneuver accuracy and maneuver measurement accuracy (via pitch down) may also be checked. Data recorded during the hold period following pitch down will provide an estimate of roll gyro drift if stars are available in both star trackers. Also a check on the accuracy of the programmed geocentric pitch rate (and/or a pitch gyro drift estimate) can be made.

Results

The Q-7 experiment was designed to obtain QI data during normal mission operations and, because special maneuvers were not allowed, all of the Q-7's performed prior to ST 1 failure were carried out in the daylight where ST data was meaningless. As a consequence there was no ST information to accurately check maneuver capability.

Horizon Tracker data indicated that they were capable of tracking the horizon throughout the maneuver range (approximately 21° in pitch for this experiment geometry). Conditions for the H/S inhibit mode have not as yet been determined from the data. Further pitch maneuver information is contained in Q-16.

Q-8 Yaw Maneuvers

Objective

Performance of the QI H/S while the vehicle is undergoing nominal yaw rates will be observed. If the maneuver is performed in the shade, more information can be obtained about potential stars within the sensitivity of the QI Star Tracker.

Results

Q-8 experiments were performed prior to and following every negative OA burn. It was established that the H/S system maintained normal tracking throughout the 180° maneuvers. Also its performance was not adversely affected by RCS thruster activity.

During yaw maneuvers pitch and roll excursions are significantly larger than during normal operation. Therefore this experiment provided an opportunity to compare QI and Barnes H/S over the greater dynamic range. Preliminary analysis shows good correlation between the two tracking systems.

In particular, Figures 11, 12 and 13 illustrate good agreement of the attitude sensors during 180° yaw arounds occurring at various times of flight (Revs 95, 242, 1408). The plots of roll and pitch attitude as dervied from the Quantic H/S on Figure 11 do not have all known corrections applied while those in Figures 12 and 13 do. Figure 11 contains a comparison between primary and redundant Barnes Sensors which also demonstrates very good agreement. Note that the Barnes (fine) telemetry saturates at one degree.

Q-9 OA Environment Test

Objective

Examine the operation of the QI experiments while in the environment of the orbit adjust. Specifically, observe if the QI H/S maintains track and if the Star Trackers can lock on to a star.

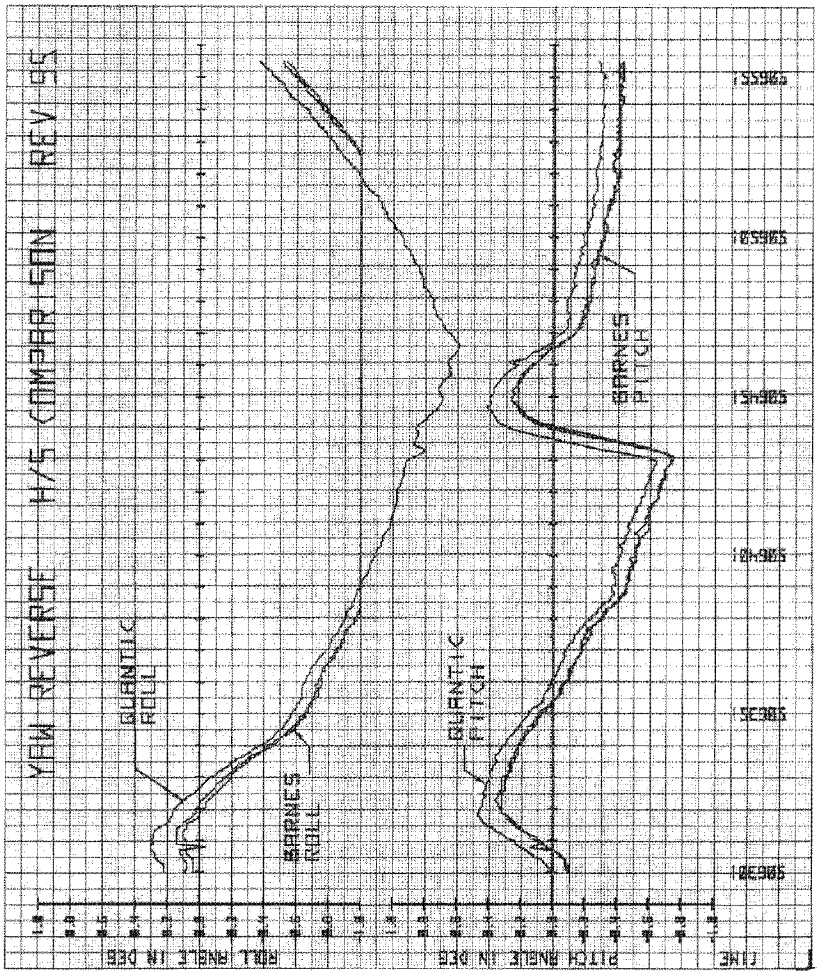

Figure 11
Yaw Reverse, H/S Comparison, Rev 95

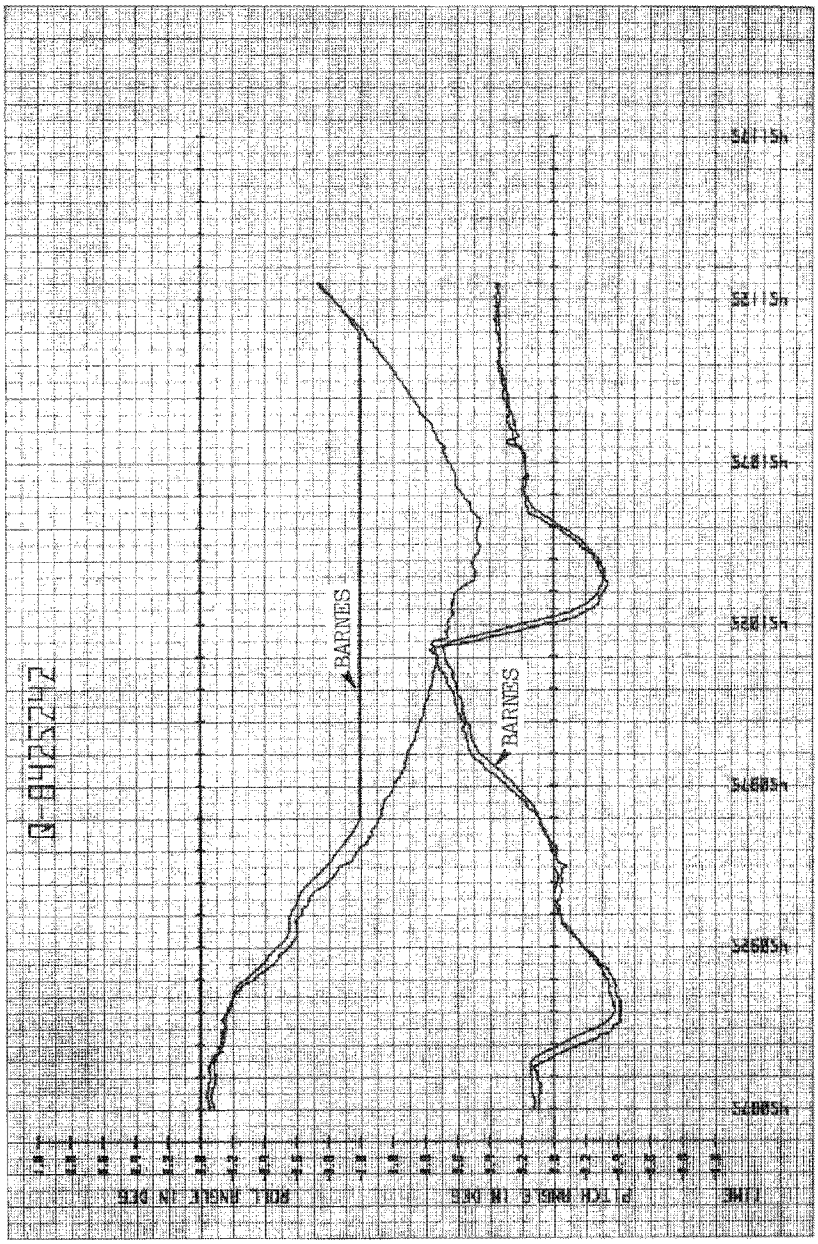

Figure 12
Yaw Reverse, H/S Comparison, Rev 242

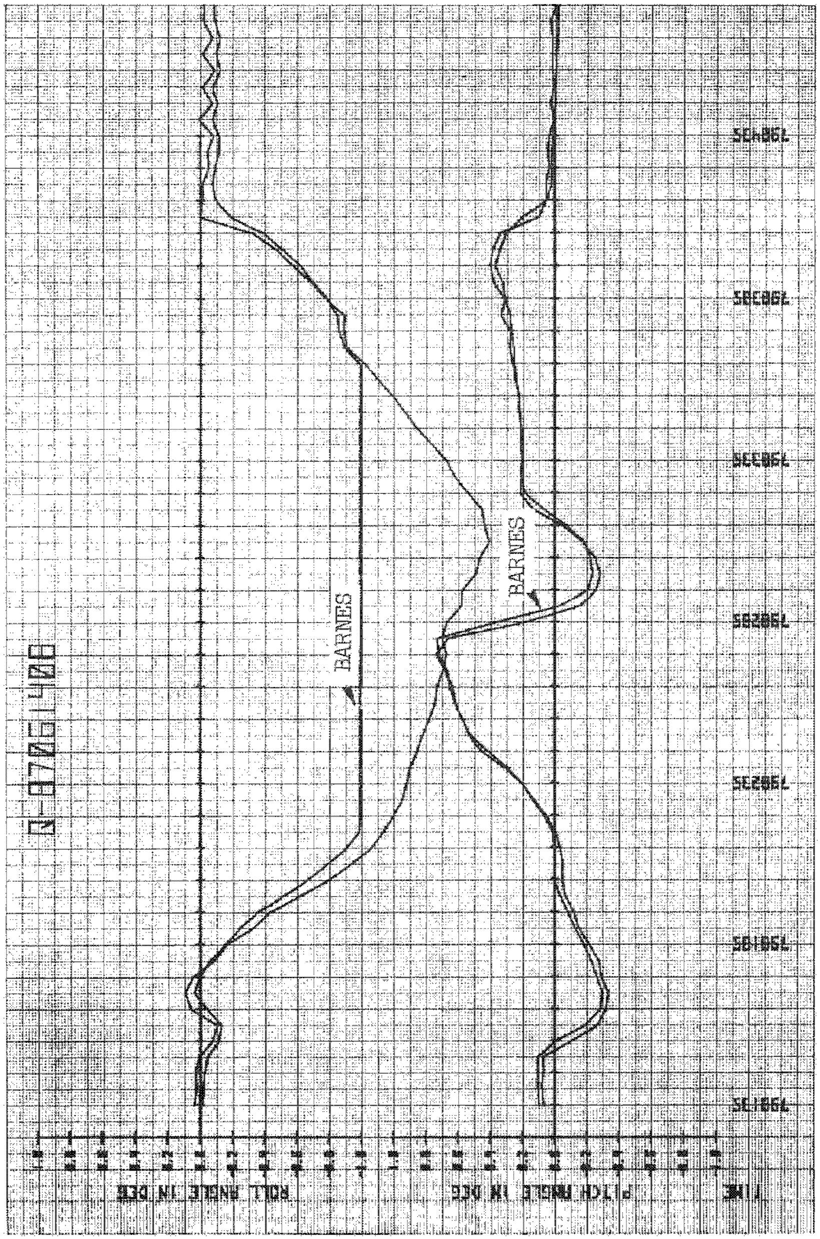

Figure 13
Yaw Reverse, H/S Comparison, Rev 1408

Results

A Q-9 experiment was conducted for all but one of the OA firings. Preliminary analysis shows no degradation in Horizon Sensor performance during an orbit adjust. Star Tracker lock-on capability during OA firings has not been evaluated as yet.

Q-10 Pitch/Roll Gyro Drift Calibration

Rationale

Determine gyro drift with QI H/S information and compare with present method of using Barnes H/S data.

Procedure

With the Quantic experiment on, fly inertially. The non-controlling Barnes H/S should also be on during this experiment.

Results

The gyro drift calibration was accomplished during Revs 1199 and 1200 with controlling system M1V1 and again during Revs 1720 through 1723 with controlling system M2V2.

Revs 1199 through 1200 will be designated experiment Q-10A. Revs 1720 through 1723 will be designated experiment Q-10B.

The following sequences were used:

Rev	Command	Vehicle Time (seconds)
1199.9	GYR1- 2-	526870.6
	Fine Mode, Geo1- 2-	526871.0
	H/S 1 DISC	526871.4
	H/S 2 DISC	526871.6
1200.9	ACS MSTCLR1-	532230.6
	ACS MSTCLR2-	532230.8
	GYR1+ 2+	532231.0
	Coarse Mode, GEO1+ GEO2+	532231.2
	H/S 1 CONN	532231.4
	H/S 2 CONN	532231.6
	Fine Mode	532390.6

Rev	Command	Vehicle Time (seconds)
1720.1	GYR1- 2-	781325.2
	Fine Mode, GE01- 2-	781325.6
	H/S 1 DISC	781326.0
	H/S 2 DISC	781326.2
1723.1	ACS MSTCLR1-	797459.2
	ACS MSTCLR2-	797459.4
	GYR1+ 2+	797459.6
	Coarse Mode, GE01+ 2+	797459.8
	H/S 1 CONN	797460.0
	H/S 2 CONN	797460.2
	Fine Mode	797619.2

Table V shows the Barnes Horizon Sensor data that are normally used to calculate gyro drift. The times were chosen at the same latitude for each individual experiment. Table VI shows the Quantic Horizon Sensor data. Table VII presents the gyro drifts which were calculated according to the following equation:

$$\text{Gyro Drift} = \frac{+\Delta \text{ INTEGRATOR } -\Delta \text{ H/S}}{\Delta \text{ TIME}}$$

Table VIII compares the gyro drifts with pre-flight data for the Barnes System.

Q-11 Prime Pylon and SV Attitude Estimation

Objective

Provide a best estimate of pylon and Satellite Vehicle (SV) attitude. The best estimate of pylon attitude will be used to calculate the expected individual horizon tracker angles for an oblate earth so that radiance effects can be inferred.

Results

This major data gathering experiment was performed at (as planned) various sun Beta angles ($\beta \approx 2°, 13°, 19°, 22°, 26°$ and $28°$) to provide indications of thermal distortion impact on experiment accuracy.

TABLE V

BARNES HORIZON SENSOR DATA

Rev	Vehicle Time (sec)	PACS				RACS			
		Barnes H/S		Integrator		Barnes H/S		Integrator	
		Pitch (deg)	Roll (deg)	Pitch (deg)	Roll (deg)	Pitch (deg)	Roll (deg)	Pitch (deg)	Roll (deg)
Q-10A									
1199	526888.0	0.8672	0.0429	-0.0610	0.0008	0.9290	0.1047	-0.0198	0.0730
1200	532217.0	0.8259	0.0429	-0.0919	-0.0095	0.8878	0.1047	-0.1125	0.0318
Q-10B									
1720	781329.6	0.0223	-0.1838	-0.0919	0.0112	0.0223	-0.1219	-0.0095	-0.1125
1721	786668.0	0.0017	0.0017	-0.0610	0.1760	0.0223	0.0429	-0.0816	0.0421
1722	792004.4	0.1047	-0.0189	0.0421	0.1039	0.0841	0.0223	-0.1125	-0.0301
1723	797339.4	0.2902	0.0017	0.2378	0.0627	0.2902	0.0635	-0.0610	-0.0713

TABLE VI

QUANTIC HORIZON SENSOR DATA

Rev	Vehicle Time (sec)	QUANTIC H/S Pitch (deg)	QUANTIC H/S Roll (deg)	PACS Pitch Integrator (deg)	PACS Roll Integrator (deg)	RACS Pitch Integrator (deg)	RACS Roll Integrator (deg)
Q-10A							
1199	526888.0	0.9438	0.1211	-0.0451	0.0150	-0.0059	0.0882
1200	532217.0	0.8925	0.1710	-0.0952	-0.0126	-0.1109	0.0262
Q-10B							
1720	581329.6	0.0940	-0.1317	-0.0922	0.0059	-0.0059	-0.1079
1721	786668.0	0.1249	0.1163	-0.0565	0.1667	-0.0730	0.0399
1722	792004.4	0.1761	0.0667	0.0372	0.0952	-0.1064	-0.0349
1723	797339.4	0.3547	0.0756	0.2317	0.0549	-0.0628	-0.0739

BIF003W/2-091480-74

SECRET / H

TABLE VII

QI/BARNES GYRO DRIFT COMPARISON

Revs	BARNES HORIZON SENSOR				QUANTIC HORIZON SENSOR			
	PACS		RACS		PACS		RACS	
	Pitch	Roll	Pitch	Roll	Pitch	Roll	Pitch	Roll
	(Degrees per Hour)							
1199 - 1200	+0.0069	-0.0069	-0.0348	-0.0278	+0.0008	-0.0524	-0.0363	-0.0758
1720 - 1721	+0.0347	-0.0139	-0.0486	-0.0069	+0.0033	-0.0588	-0.0660	-0.0676
1721 - 1722	0	-0.0348	-0.0626	-0.0348	+0.0287	-0.0148	-0.0571	+0.0368
1722 - 1723	+0.0070	-0.0417	-0.1043	-0.0556	+0.0609	-0.0332	-0.0911	-0.0323
*1720 - 1723	+0.0139	-0.0301	-0.0718	-0.0324	+0.0142	-0.0356	-0.0714	-0.0390

* Note, the values more closely correlate when the longer time span is used because system instrumentation errors become less significant.

SECRET / H

BIF003W/2-091480-74

Approved for Release: 2025/06/18 C05137285

TABLE VIII

BARNES GYRO DRIFT COMPARISON

Data Source	PACS		RACS	
	Pitch (°/Hr)	Roll (°/Hr)	Pitch (°/Hr)	Roll (°/Hr)
Vendor Data Pre-Environmental Results	-0.12	+0.049	+0.047	-0.065
Vendor Data Post Environmental Results	-0.112	+0.070	+0.031	-0.028
Module Test	-0.17	0	+0.03	-0.06
Revs 1720 - 1723 (average)	+0.0141	-0.0329	-0.0716	-0.0357

SECRET / H

Approved for Release: 2025/06/18 C05137285

Unfortunately the failure of ST 1 on Rev 454 impaired the accuracy with which the Horizon Tracker performace can be evaluated. Preliminary data evaluation for the Q-11 (Rev 308/309) indicates good agreement between attitude estimates derived from Barnes and QI Horizon Sensors around a full rev. It also indicates very good agreement between attitude estimates derived from the QI H/S and the QI Star Trackers (during the shadow). Correlation of Barnes and QI performance data taken from several Q-11 experiments throughout the flight show that there may be a sun Beta angle effect (thermal distortion ARM-to-pylon) on the accuracy comparison between H/S systems. This can be seen in Figures 14 and 15 which are plots of pitch and roll attitude for a full orbit on Revs 308 ($\beta = 2°$) and 1637 ($\beta = 26°$). In order to indicate the comparison in more detail, the difference (QI-Barnes) between the corresponding attitude estimates are plotted in Figures 16 and 17. It is apparent that the mean of the difference has shifted about 0.05 degrees.

Q-12 Secondary SV and Pylon Attitude Estimation

This sub-experiment was cancelled and superseded with Q-11.

Q-13 Low Frequency Horizon Radiance

Objective

After removal of fixed relative biases between the Barnes H/S pitch/roll estimates and the derived Quantic H/S pitch/roll estimates, a comparison of the residual estimates of the two sensors can be made.

Results

Several of these experiments were performed during the primary mission for abbreviated periods (2 revs). During solo a six rev nose forward test was done successfully. However, the nose aft test data was impaired because one Quantic Horizon Tracker was hung up on its upper limit due to a previous maneuvering test.

The data gathered during this experiment may not necessarily be analyzed at present but is available for investigations into low frequency radiance effects.

SECRET / H

BIF003W/2-091480-74

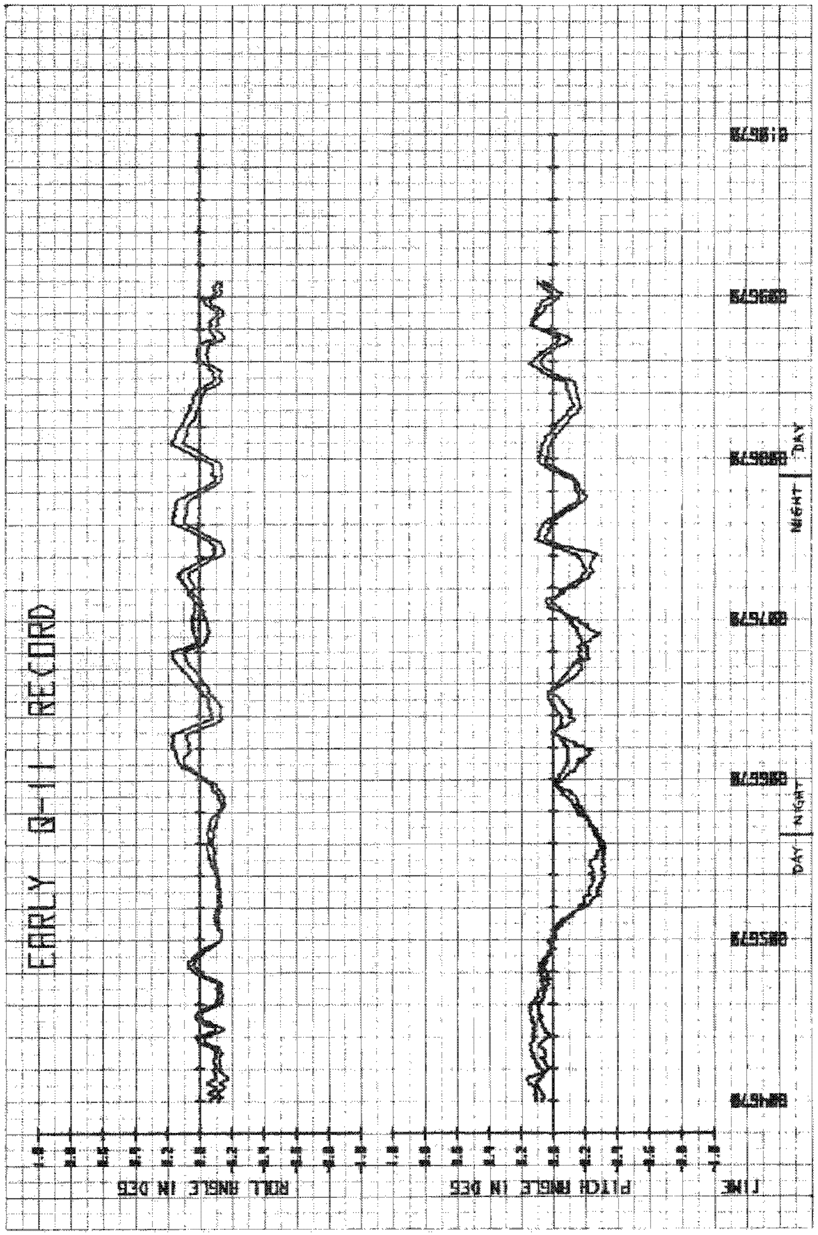

Figure 14
Quantic and Barnes Pitch and Roll Attitude, Rev 308

SECRET / H

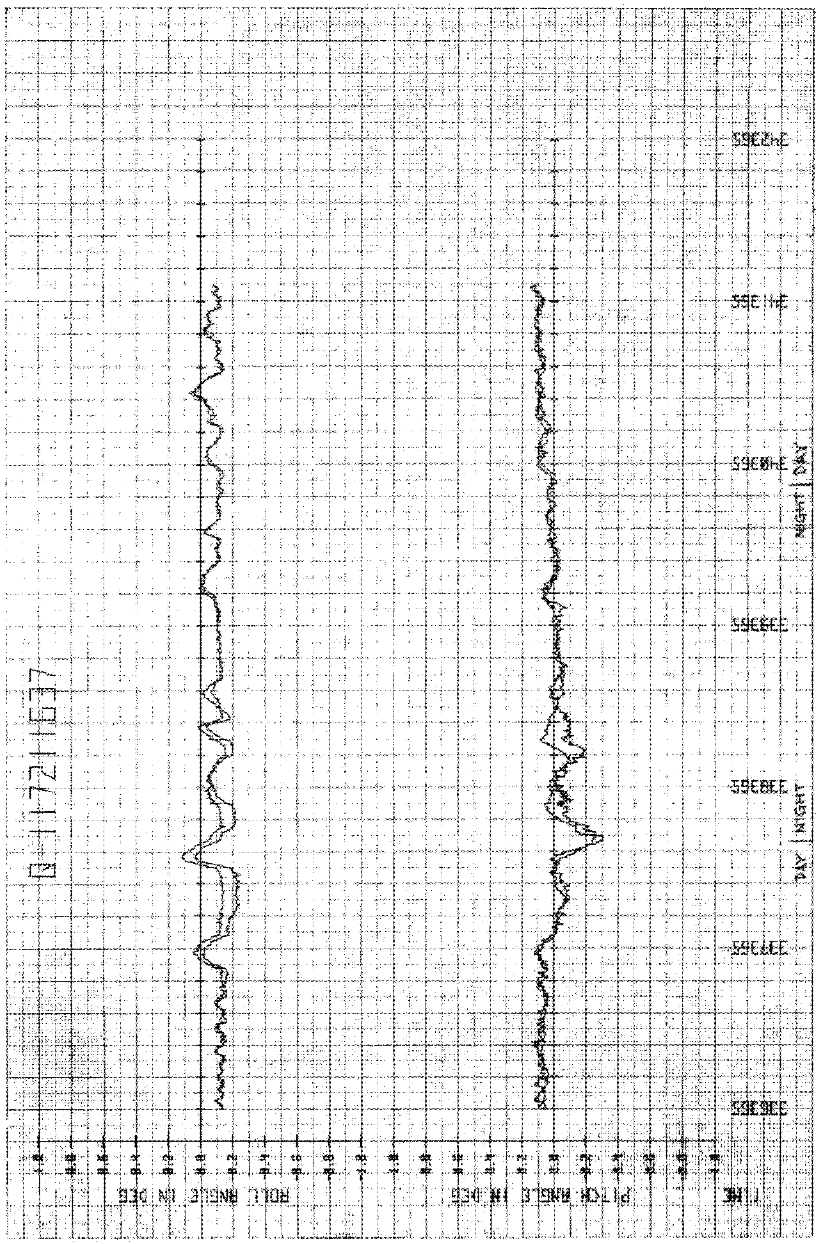

Figure 15

Quantic and Barnes Pitch and Roll Attitude, Rev 1637

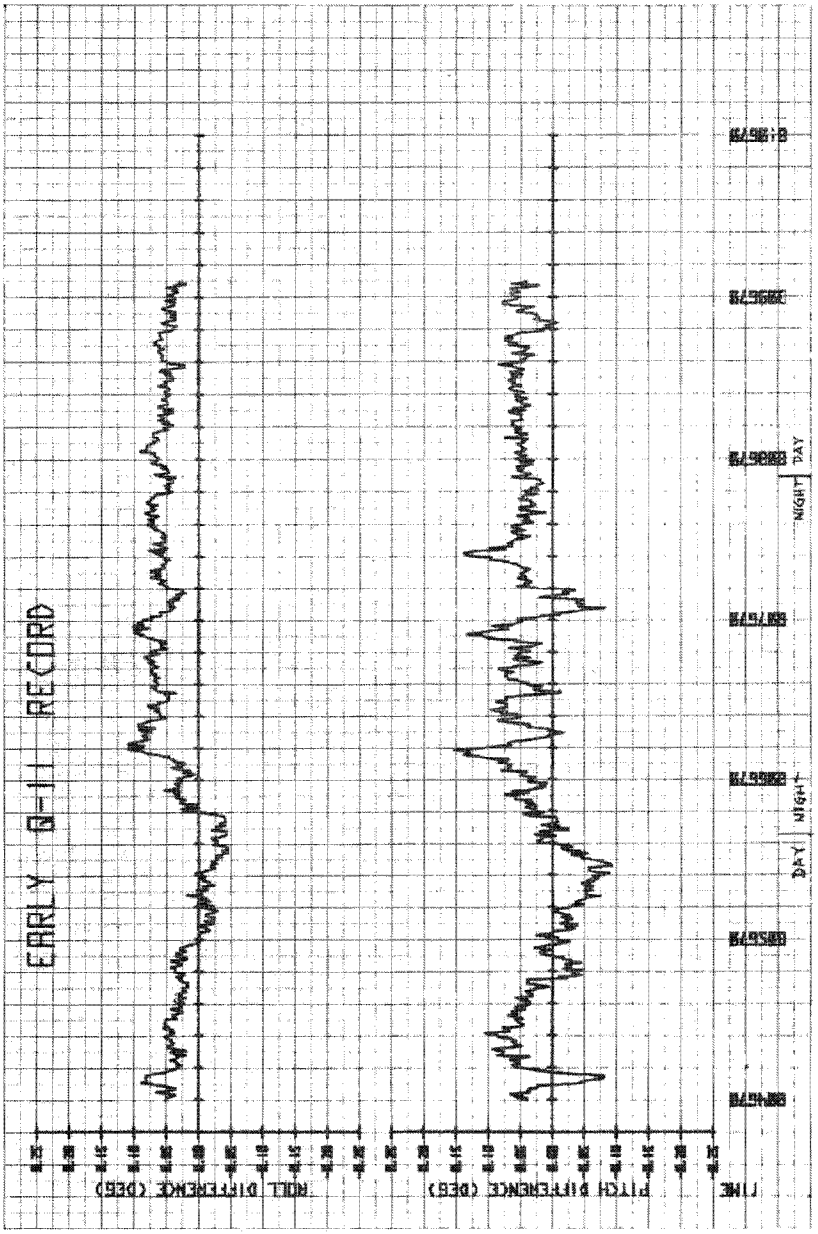

Figure 16

Quantic Minus Barnes Attitude Difference, Rev 308

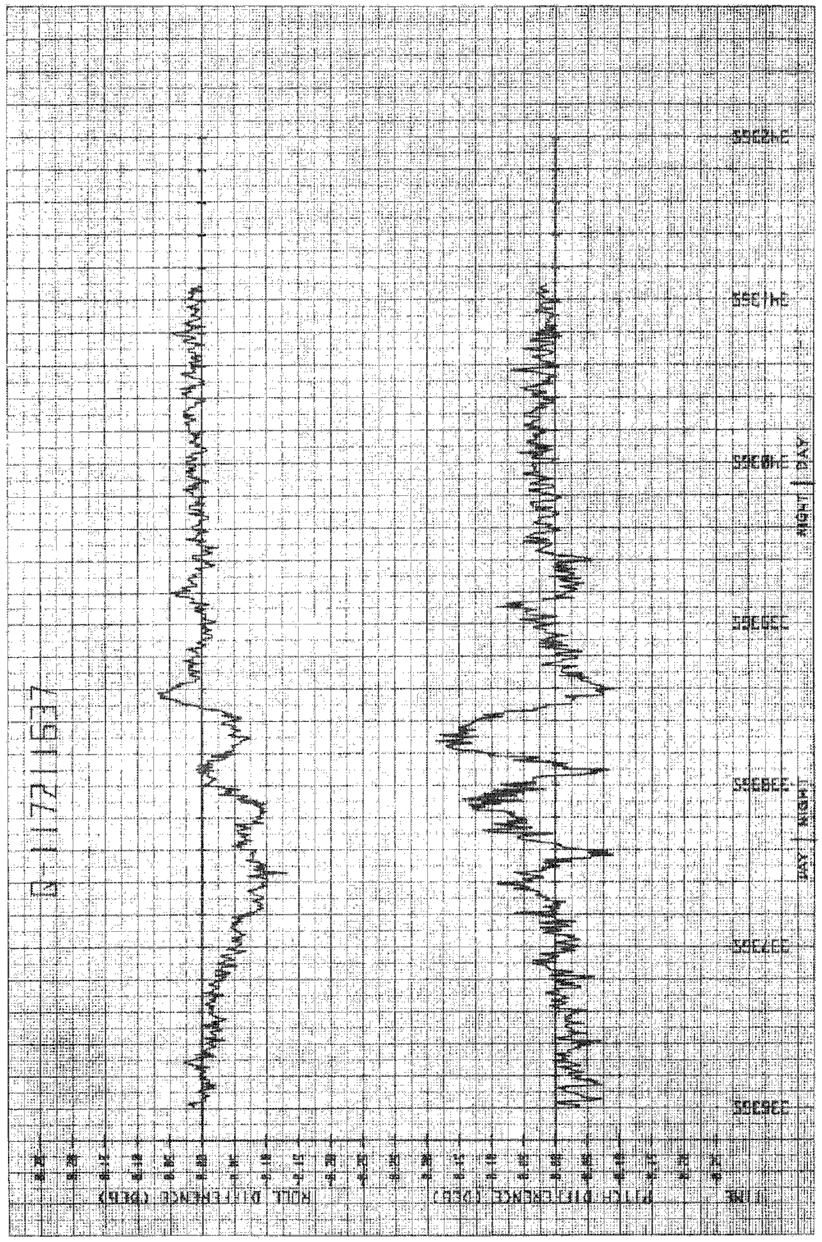

Figure 17
Quantic Minus Barnes Attitude Difference, Rev 1637

Q-14 Rate Integration Check

Objective

Compare integration of gyro rates with the control system integrators versus the ground integrations.

Results

This experiment was done in conjunction with Q-10. The data is to be used as a validation of the Phase II (final phase of data reduction) data processing filter. This work has not been completed as yet.

Q-15 Relative Star Tracker to Star Tracker Bias

This experiment was cancelled due to the failure of ST 1 on Rev 454.

Q-16A Pitch Maneuver Calibration

Objective

To calibrate STC mode pitch maneuver indicator (PDWN), and the Quantic HS large angle (pitch) accuracy as well as the vehicle pitch maneuver accuracy.

Results

On Rev 1632 a negative pitch maneuver was performed with the following sequence:

COMMAND	SYSTEM TIME (SEC)	VEHICLE TIME (SEC)
H/S 2 DISC	53579.1	318237.6
GYR2-	53579.5	318238.0
PITCH NEGATIVE	53579.9	318238.4
STOP MANEUVER	53609.5	318268.0

The pitch attitude was 0.0 degree at vehicle time 318238.4 seconds.

Therefore, $\theta = +\Delta\theta_{INTEGRATOR} + |\Delta R| -0.068667\ \Delta + -0.705191 \times 29.6.$

Pitch gyro drift is negligible within a span of 150 seconds. Figure 18 shows PDWN, the Quantic H/S pitch attitude and the calculated θ. Table IX compares the pitch attitudes.

TABLE IX

PITCH ATTITUDE COMPARISON

Vehicle Time (sec)	Calculated* (deg)	PDWN (deg)	Quantic H/S (deg)
318288.6	-21.0	-20.3	-21.2
318338.6	-21.0	-20.3	-21.2
318388.6	-21.0	-20.4	-21.3

*Note that this calculated pitch angle is an after the fact calculation and contains information that is normally not known prior to commanding the maneuver. In particular, the change in the pitch integrator state ($\Delta\Theta$ integrator) will not be known apriori. However, the relative change in orbit frame position (actual-programmed) could be accounted for by use of predicted ephemeris.

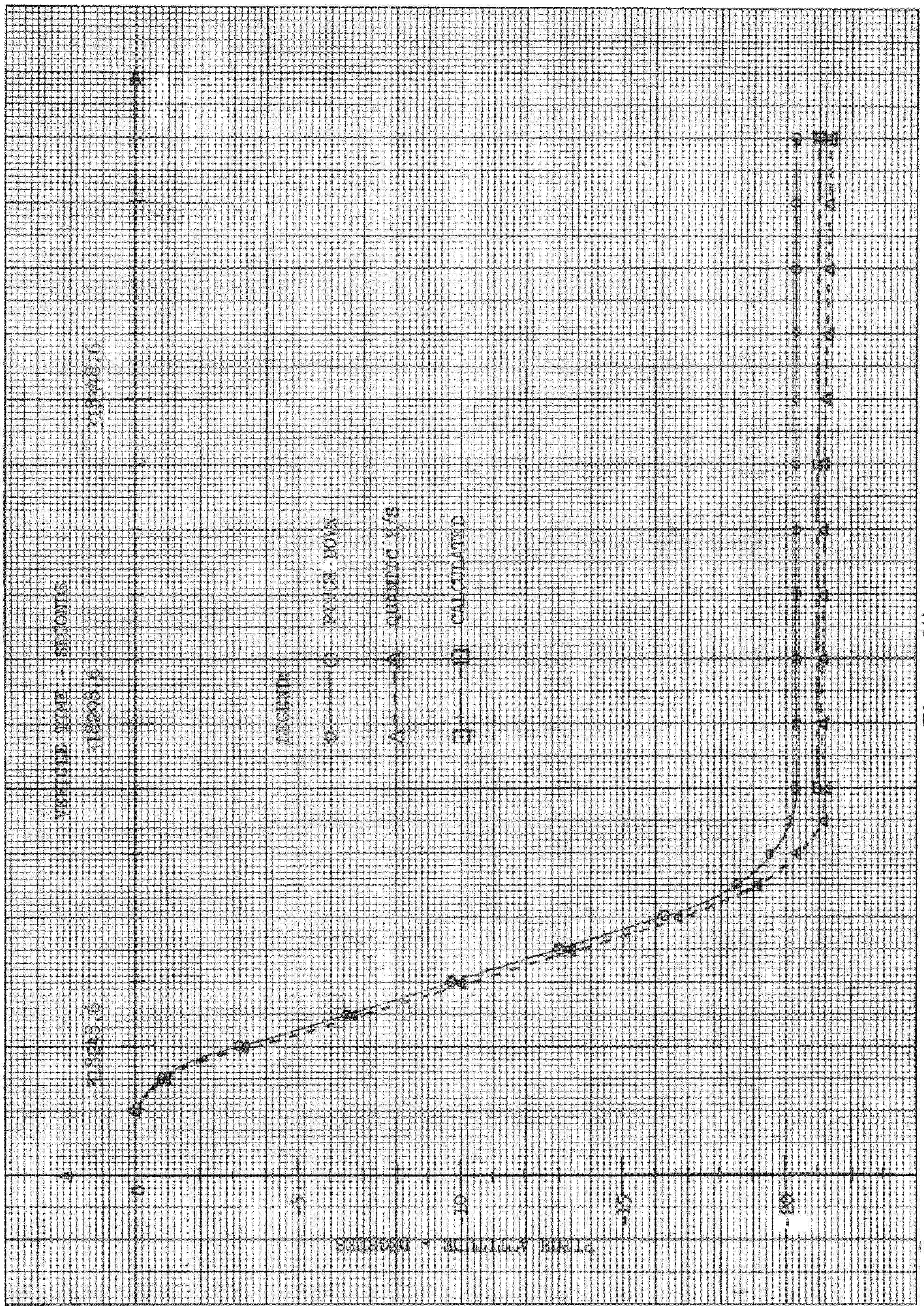

Figure 18
Pitch Attitude Versus Time

Results

Originally, calibration of vehicle pitch maneuvers was to be done using the STS. Due to the failure of ST 1 prior to conducting this experiment, the calibration technique had to be modified but preliminary data evaluation based on ST 2 proved to be a reasonable verification of pitch maneuver accuracy. As shown in Table IX a pitch maneuver of -21.0° was programmed (calculated). Three independent measurements (PDWN, QI HS, and QI ST 2) were made with respective values of -20.3, -21.2 and -20.95 degrees. These values indicate that vehicle capability for pitch maneuver accuracy is at least an order of magnitude better than specification requirements.

These measurements also show that PDWN presents a fairly accurate indication of maneuver performance provided that no telemetry data drop outs occur during the maneuver.

The QI HS large angle measuring capability was of specific interest since it was to be used in a later experiment (Q-21). As the data in Figure 18 indicates the HS as configured for this experiment had a dynamic range capability slightly beyond 21° with good accuracy over the range.

Q-16B Roll Maneuver Calibration

Objective

To determine the accuracy with which inertial roll maneuvers may be performed.

Results

Some data analysis remains to be done on this experiment but preliminary indications are that vehicle performance in roll maneuver accuracy is as good as pitch maneuver accuracy (Q-16A). Preliminary numbers are as follows:

	+ ROLL	- ROLL
Programmed	+9.811	-9.801
Q-S/T	+9.810	-9.845

Q-17A Roll HS Inhibit

Objectives

The primary objective of this experiment was to establish the roll angle inhibit point for QI HSS. A secondary objective was to determine relative alignment between the ARM and main pylon roll planes. A tertiary objective was to obtain information about horizon radiance profile if possible.

Results

This test was carried out by continuously rolling the vehicle for one rev (Rev 1738) while continuously operating tape recorders. The data has not been analyzed as yet.

Q-17B Pitch HS Inhibit

Objectives

The primary objective of this experiment was to establish the pitch angle inhibit point for the QI HS. A secondary objective was to determine relative alignment between the ARM and main pylon pitch planes.

Results

This test was carried out by continuously pitching the vehicle through 635.4 degrees on Rev 1714. This maneuver was followed by a 180 degree roll maneuver which left the vehicle in a nose aft local horizontal position for tests which followed (Q-11, Q-13). Coming out of this large angle maneuver, one of the HT's on the main pylon was hung up in its upper limit. This condition had an impact on the subsequent tests which followed (Q-11, Q-13) before an HT search command could be sent to release it. The detailed data analysis relative to HS pitch inhibit angles and pitch plane alignments has not yet been completed.

Q-18 Best Bet Attitude

Objective

To evaluate attitude comparison data between Barnes HS, QI HS and QI ST Systems for several consecutive revs.

Results

The data from this experiment has not been analyzed as yet.

Q-19 Magnetometer Calibration

Objective

Compare attitude estimates from the LB II magnetometers with attitude measurements of the QI experiment.

Results

Figure 19 compares magnetometer outputs with DGMAP theoretical magnetometer outputs at various latitudes around the orbit. The number of data points for P and R sensors is limited due to telemetry saturation.

The data shows that although the magnetometer has some errors introduced by induced magnetism it is well within the allocated error for distortion.

For correlation of magnetometer data with QI and Barnes data refer to Experiment Q-21.

Q-20A Sun Impingement - ST 2

Objective

To determine if ST design was adequate to withstand full sun in the field of view.

Results

Due to relative sun vector motion (non-sun synchronous) on SV-8 the sun passed through ST 2 FOV on every rev from about 26 June through deboost. No deleterious effects were noted. Detailed data was collected and analyzed for several different revs where impingement could have occurred. In every instance the ST mirror appeared to track a sun glint which prevented full sun impingement on the ST detector. Thus the solar protection feature of the ST was not tested and cannot be evaluated.

Q-20B Sun Impingement - HS 2 (Small Pylon)

Objective

The QI HS design includes a sun sensing element and associated circuitry which depresses the sensor away from the sun and toward the earth when the sun approaches the FOV. This feature protects the radiance detector from possible damage due to direct sun

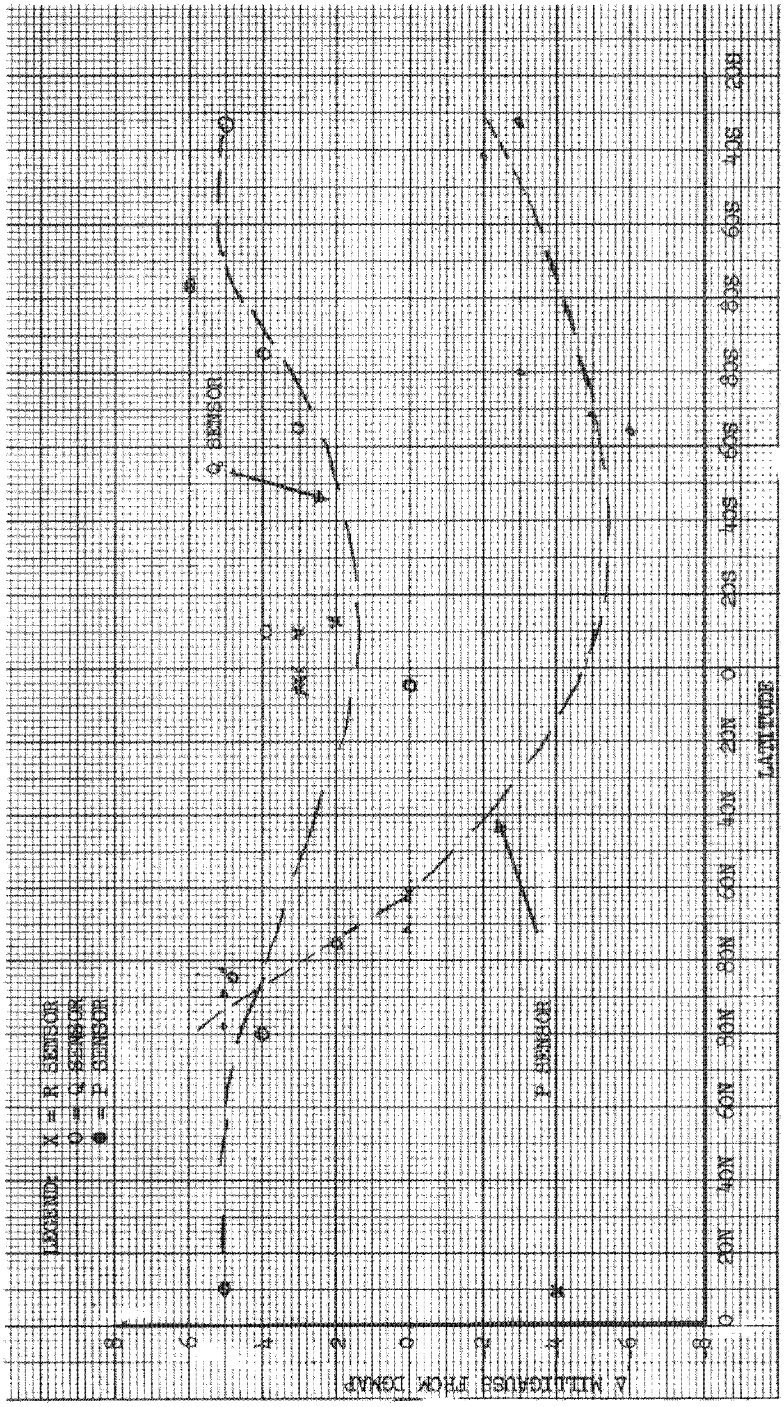

Figure 19

Magnetometer Differences from 'DG MAP for Different Latitudes impingement. This experiment was performed to demonstrate the operation of the sun sensor.

Results

This experiment was carried out on Rev 1718 by performing a yaw maneuver from a nose aft attitude prior to sunrise. This placed the FOV of HT 2 on the horizon at a point where it would see the sun at orbital sunrise. The data shows the HT angle depressing 3.5 degrees below the horizon as the sun approaches the FOV and its recovery as the sun recedes. This verifies the successful performance of the sun sensor.

Q-21 LB Attitude Estimation

Objective

Use QI HSS to measure attitude pointing capability of the LB system while operating in the RV mode. The experiment version of the Quantic HSS has a readout range large enough (approximately 21°) to allow it to measure vehicle attitude during a typical LB operation. The Barnes HSS readout telemetry is limited to ±10 degrees.

Results

This experiment was performed on Rev 1751. The ACS was deactivated at t = 80 seconds. At t = 0 seconds, Lifeboat Execute was commanded while in the North-South, RV Mode. At t = 360 seconds Lifeboat was reset and control was subsequently returned to ACS.

At the time of Lifeboat reset the vehicle attitude was -17.49 degrees in pitch and 0.54 degrees in roll as determined by the Quantic Horizon Sensor. Yaw attitude determined by integrating the ACS yaw gyro rate was approximately -2.5 degrees.

These attitudes are well within the Lifeboat specification which requires the vehicle X-Y plane to the earth's magnetic field vector be perpendicular within ±7.5 degrees in the latitudes and longitudes at which this experiment was conducted. Table X is a summary of pitch and roll attitudes determined by magnetometer and by horizon sensors.

A plot of pitch attitude during Lifeboat control is shown in Figure 20. Pitch attitudes determined by: (1) calculating pitch attitude based on the

SECRET / H

TABLE X

COMPARISON OF PITCH AND ROLL ATTITUDES

Time (sec)	'DG MAP P (mg)	D202 P (mg)	ΔP (mg)	DG H (mg)	Deg Per mg	Deg Calc. Pitch Angle	Quantic HSA Pitch (deg)	Barnes HSA Pitch (deg)	'DG MAP Q (mg)	D201* Q (mg)	ΔQ (mg)	Deg Calc. Roll Angle	Quantic HSA Roll (deg)	Barnes HSA Roll (deg)
[illegible]	3.2	6	2.8	530	0.108	- 0.3	- 0.13	0.04	- 8.8	- 7	1.8	0.2	-0.13	-0.2
[illegible]	-47.7	-38	3.7	536	0.107	- 0.4	- 0.13	0.02	-10.4	-10	0.4	0.04	-0.13	-0.34
[illegible]	-59.3	-38	21.3	536	0.107	- 2.3	- 1.90	-1.8	-11	- 4	7	0.7	0.53	0.1
[illegible]	-103.9	-41	62.9	527	0.109	- 6.9	- 6.93	-6.8	-12.4	- 1	11.4	1.2	1.04	0.9
[illegible]	-125.6	-41	84.6	519	0.110	- 9.3	- 9.36	-9.0	-13.1	- 1	12.4	1.4	0.92	1.2
[illegible]	-146.2	-32	114.2	508	0.113	-12.9	-13.58	---	-13.9	- 1	12.9	1.5	1.47	1.2
[illegible]	-175.3	-23	152.3	486	0.118	-17.9	-17.49	---	-15.2	-10	5.2	0.6	0.54	0.8

* D201 corrected for -4 mg instrumentation bias.

BIF003W/2-09480-74

SECRET / H

Approved for Release: 2025/06/18 C05137285

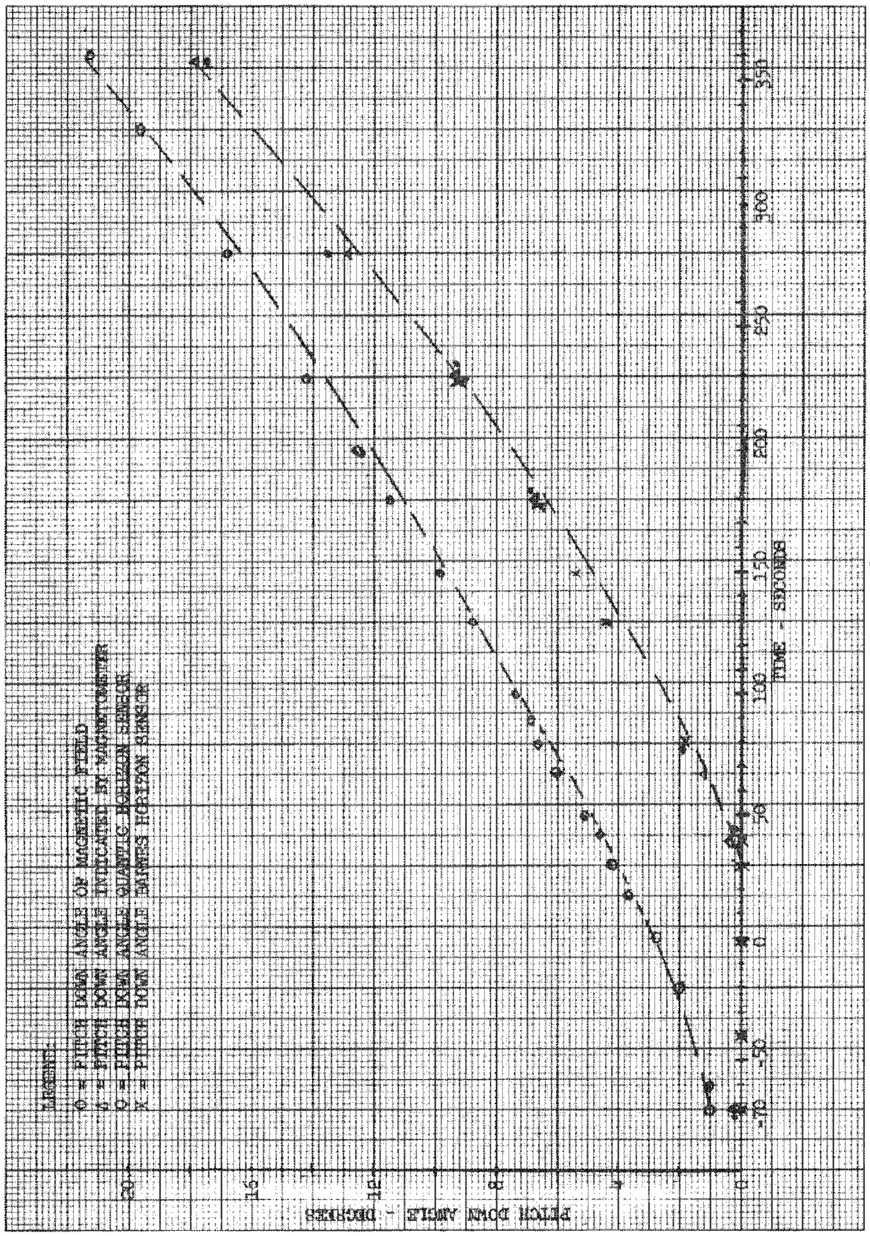

Figure 20
Pitch Down Angles

deviation of the P magnetometer sensor reading from DG MAP, (2) Barnes Horizon Sensor and (3) Quantic Horizon Sensor are plotted.

The maximum deviation between the pitch attitude determined by the magnetometer and by the horizon sensors was 0.7 degree.

The deviation of the pitch attitude from the theoretical pitch angle is also shown in Figure 20. The theoretical pitch angle is the angle of the earth's magnetic vector, H, with respect to local horizontal. The field vector pitch angle at the time of RV simulation was -20.4 degrees. The measured pitch angle was -16.8 degrees.

Figure 21 is a phase plane plot of P magnetometer readings and pitch axis rate. The relation of the magnetic field vector and the vehicle axes was such that both the magnetometers were well within dead band at the time of Lifeboat Execute. Consequently no large rates or attitude errors were observed.

Thrust valve firing was negligible consisting of 3 pulses of 24 milliseconds each of Thrust Valve 2.

Roll attitude error and rate were small and were never large enough to cause thrust valve firing. This is in agreement with predictions based on 'DG MAP. The maximum deviation between the roll attitude determined by the magnetometer and by the horizon sensors was 0.6 degree. The measured roll attitude at the time of RV simulation was 1.0 degree.

Yaw attitude is not controlled or specified. Yaw rates were small and never approached the dead band. Therefore, no thrust valve firings were required for yaw corrections either.

<u>Q-22 Sequential Maneuver Calibration</u>

<u>Objective</u>

The purpose of this experiment was to determine if any in-plane (scan plane) shift occurred between the ST Sensors and ARM due to the ascent environment.

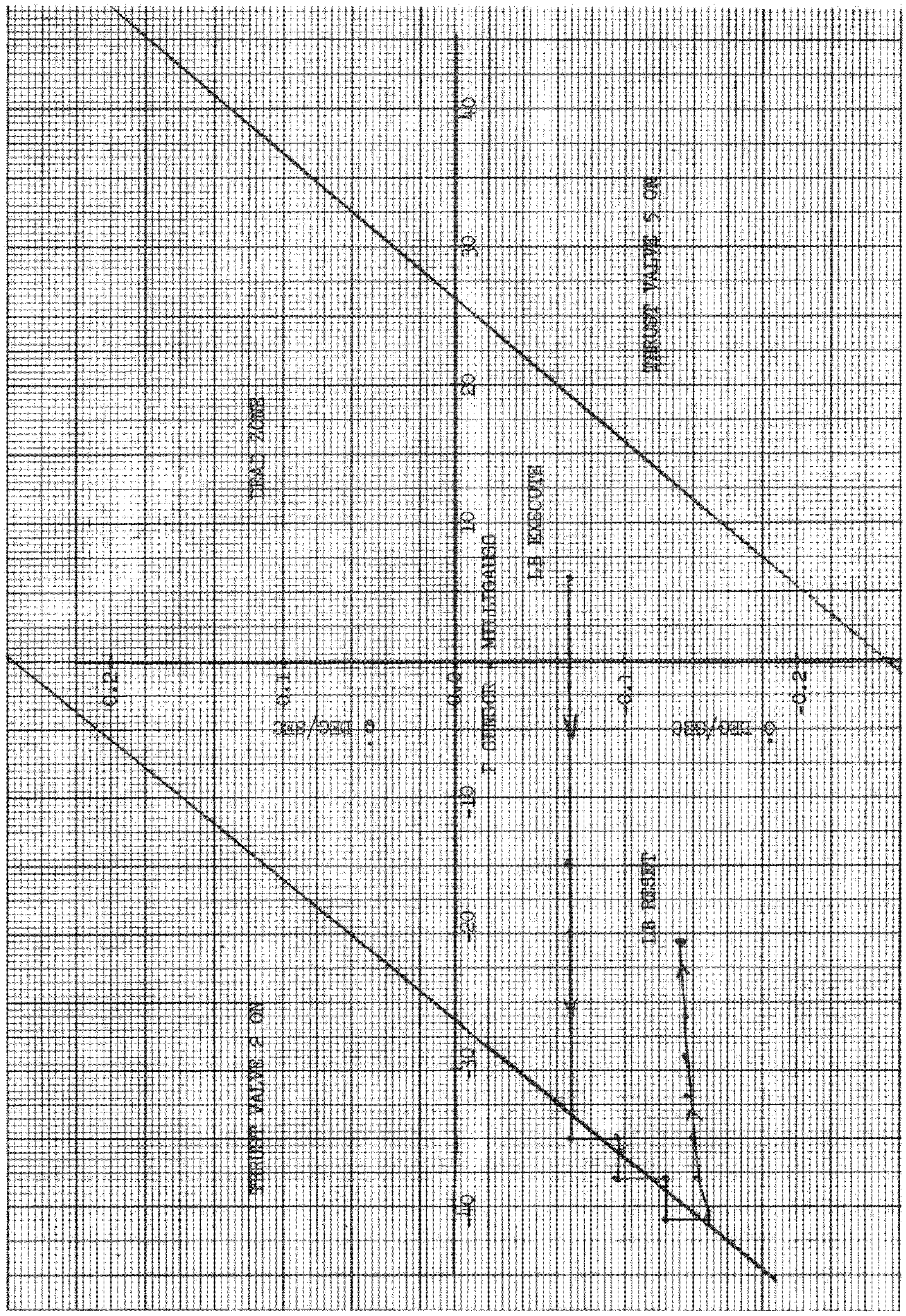

Figure 21
Phase Plane Pitch Rate Versus Pitch Attitude

Results

This experiment was conducted on Rev 1704. The method used to invert the star sighting within the ST FOV was to pitch up 19°, roll right 143° and a pitch up of 160°. A preliminary analysis of the data shows that the in-plane alignment was different from the ground test reference measurement by 0.005°.

The error sources involved in this calculation have not been assessed as yet and will undoubtedly have some effect on the confidence limits associated with this measurement.

Also thermal distortion effects will be indistinguishable from the misalignment due to ascent shifting.

Q-23 Gyro Reference Plane Calibration

Objective

Determine the relative alignment between the large pylon and ARM yaw planes.

Results

The experiment was accomplished on Rev 1747 by inertially maneuvering the vehicle through 720 degrees of yaw on the dark side of the orbit.

The data has not been analyzed as yet.

Q-24 Geocentric Rate Determination

Objective

Use the Quantic experiment to measure the digital geocentric program rate. With the Quantic experiment on, disconnect the Barnes H/S while leaving the geocentric rate connected and the control system in fine mode. Maintain this configuration for two continuous revs.

Results

The geocentric rate determination began on Rev 1733.6 with M2V2 the controlling system. The sequence used in this test was as follows:

COMMAND	VEHICLE TIME (SECONDS)
H/S 2 DISC	14343.6
GYR-	14343.8
COARSE MODE	25033.4
H/S 2 CONN	25033.8
GYR+	25034.0
FINE MODE	25633.4

Table XI shows the data for four time points when the gyrocompassing is stopped and horizon sensors are disconnected.

The equation to determine the magnitude of the geocentric program rate follows:

$$\text{Geocentric Program Rate} = 360° + \frac{\Delta\Theta_I - \Delta\Theta_{H/S}}{\text{REV TIME}} - \text{Gyro Drift Rate}$$

The gyro drift rate during Revs 1720 through 1723 was -0.00002 degrees/seconds. The geocentric program rate was calculated to be 0.06865°/sec from Rev 1733 through 1734 and 0.06867°/sec, from Rev 1734 to Rev 1735 which averages to 0.06866°/second. This is in close correlation to the last ground hardware test which measured the geocentric program rate as 0.068667°/second.

<u>Q-25 Quantic Star Tracker 1 Health Check</u>

<u>Objective</u>

Determine if any self healing had occurred to ST 1 during the 82 day "off" period and to determine if Star Tracker 1 anomaly will affect Star Tracker 2 operation if Head 1 is left on.

Part I - With all of the Quantic System on except for Star Tracker 1 turn on Star Tracker Head 1 for 60 seconds over a station pass, then turn off total Quantic system. On the next station pass, turn on the total Quantic System except Star Tracker Head 1. If system has not been degraded continue operations with ST 1 off until Part II is initiated.

Part II - After completing all critical Quantic experiments, turn on ST 1 and leave on. Determine if reset of system is affected by leaving S/T Head 1 on.

TABLE XI

ATTITUDE DATA FOR Q-24

Rev	Latitude	Vehicle Time (sec)	Quantic H/S Attitude ($\Theta_{H/S}$) (deg)	Estimated Integrator Attitude (Θ_I) (deg)
1733	0°	16773.8	-4.1835	-0.0137
1734	0°	22102.8	-10.0203	-0.1233
1734	0°	19415.8	-5.8121	0.1031
1735	0°	24744.8	-11.6489	0.1039

Results

Time of experiments were as follows:

Part I	Date	System Time	Vehicle Time
Start	July 27, 1974	68196.8	98794.4
Stop	July 27, 1974	68256.8	98854.4
Part II			
Start	July 28, 1974	66750.1	183747.8
Stop	July 28, 1974	81954.5	198952.2

ST 1 failed to turn on on both tests. ST 1 CEU voltage remained at the failed value of 2.80 telemetry volts. No adverse effect was noted on ST 2 operation during either part of this test.

Figure 22 is a plot of star tracker angles from Part I of the test. Figures 23 and 24 are plots of star tracker angles from the beginning and end of Part II of the test. As can be seen from Figures 22 and 24 ST 2 shows a dither at the ends of the scan range. Figure 25 shows that this dither was occurring prior to this test and is unrelated to the S/T 1 failure.

On all the figures, an asterisk (*) indicates a valid star sighting. Every asterisk had a star sighting time, a star indicated on Bit 14 of the time word and a star brightness indication. This was true of both Star Trackers.

On Figure 24, Star Tracker 2 shows "bad" angle outputs at times 198877 and 198879. Associated with these bad angle readings were star indications as noted above. However, Bit 14 of the angle output did not indicate a radiance event as it had in all other star sightings. In both cases the "bad" angle output was approximately -3.5 degrees. The cause of the bad readings have not been investigated as yet.

Q-25 Test Rev 1765

* Indicates star event with brightness outputs.

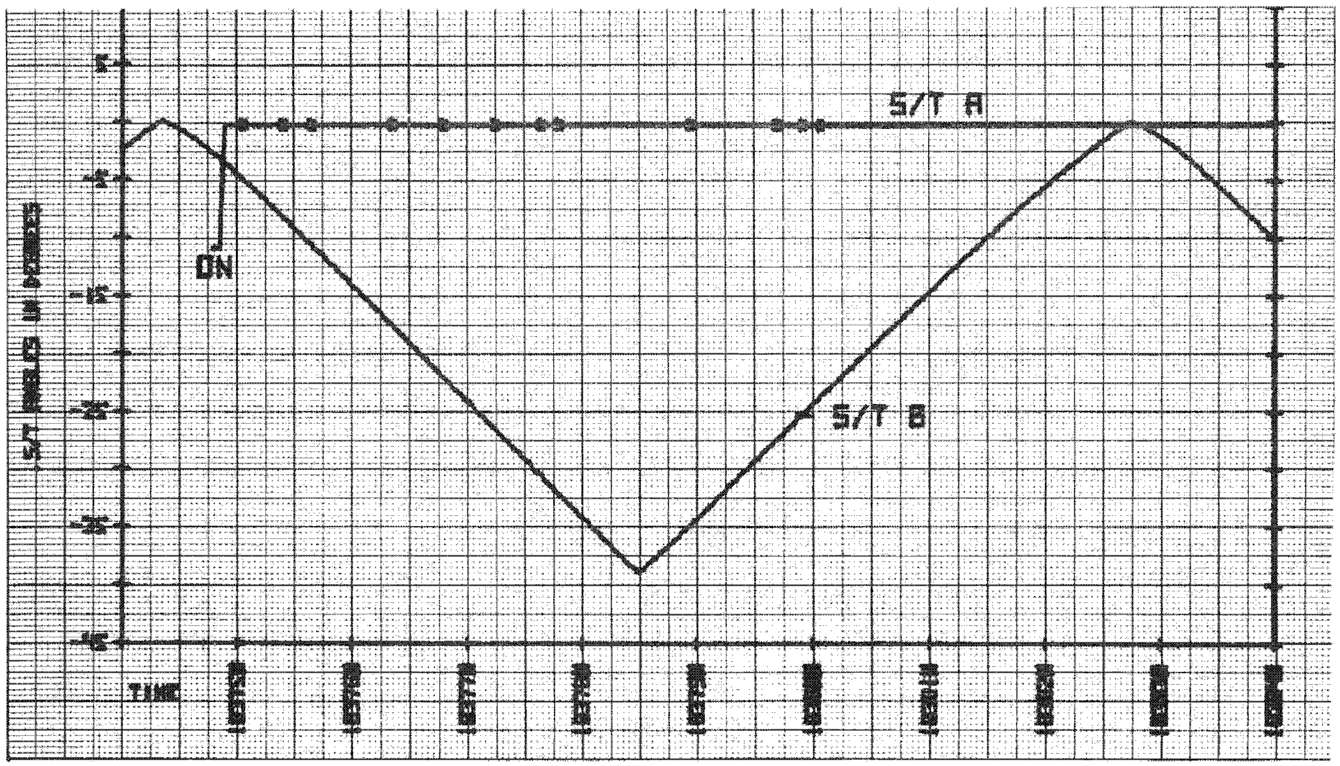

Figure 22

Star Tracker Angles, Part I

Approved for Release: 2025/06/18 C05137285

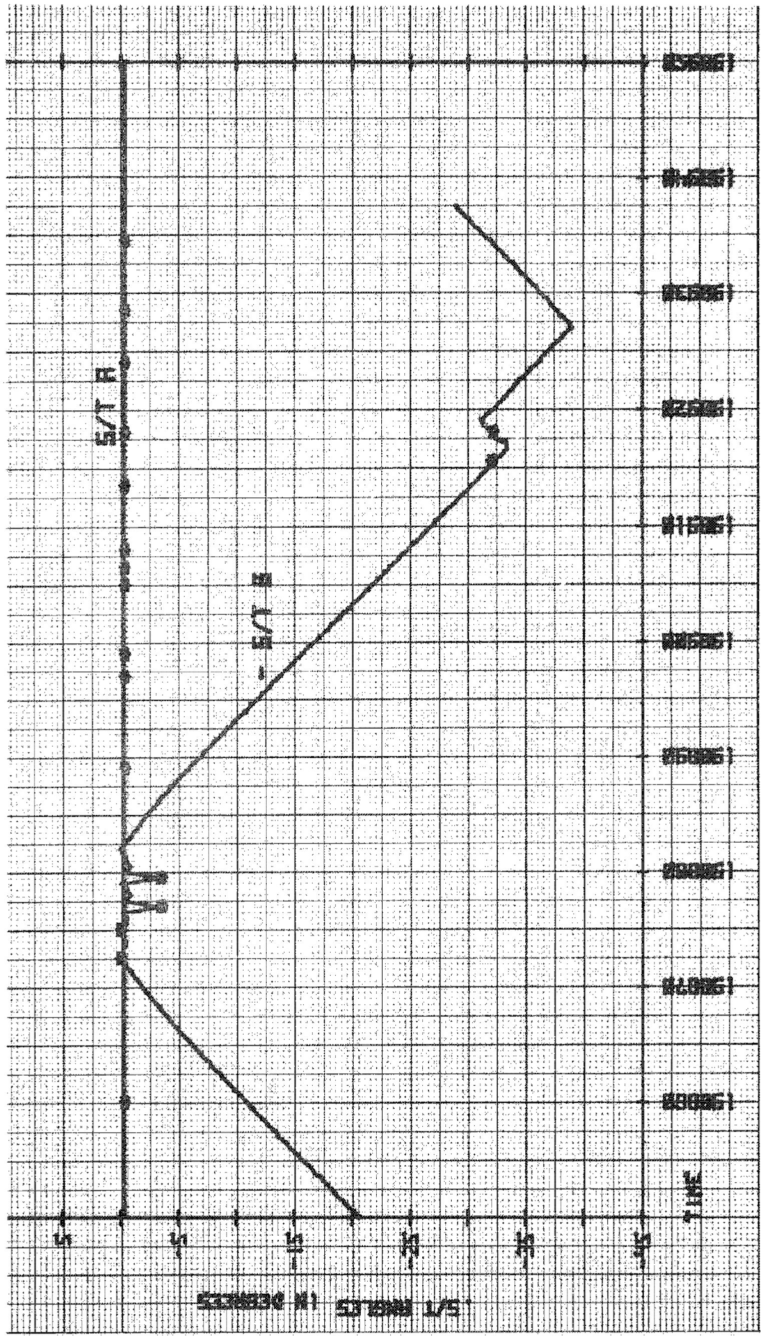

Q-25 Test, Rev 1768

* Indicates star event with brightness outputs.

Figure 23

Star Tracker Angles, Part II

Q-25 Test (S/T A On 98794)

* Indicates radiance event showing star.

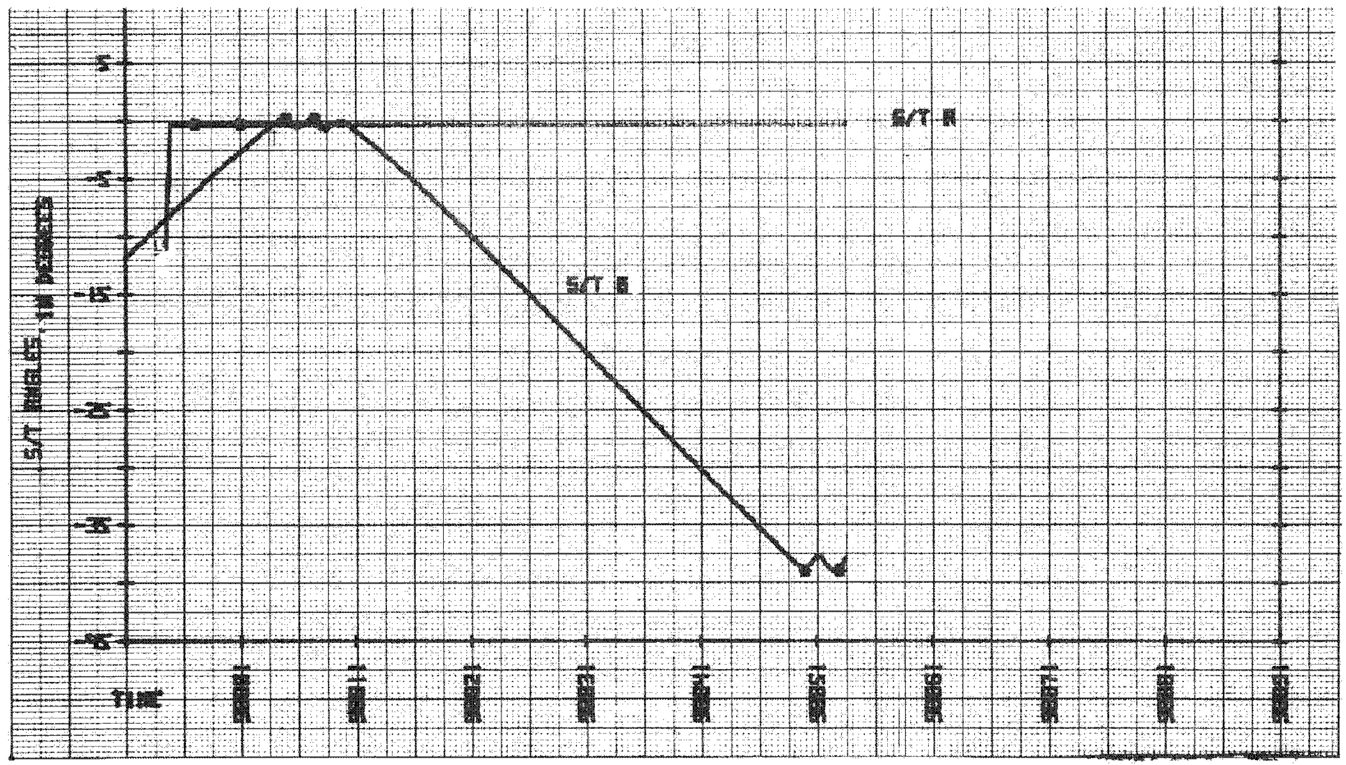

Figure 24

Star Tracker Angles, Part II

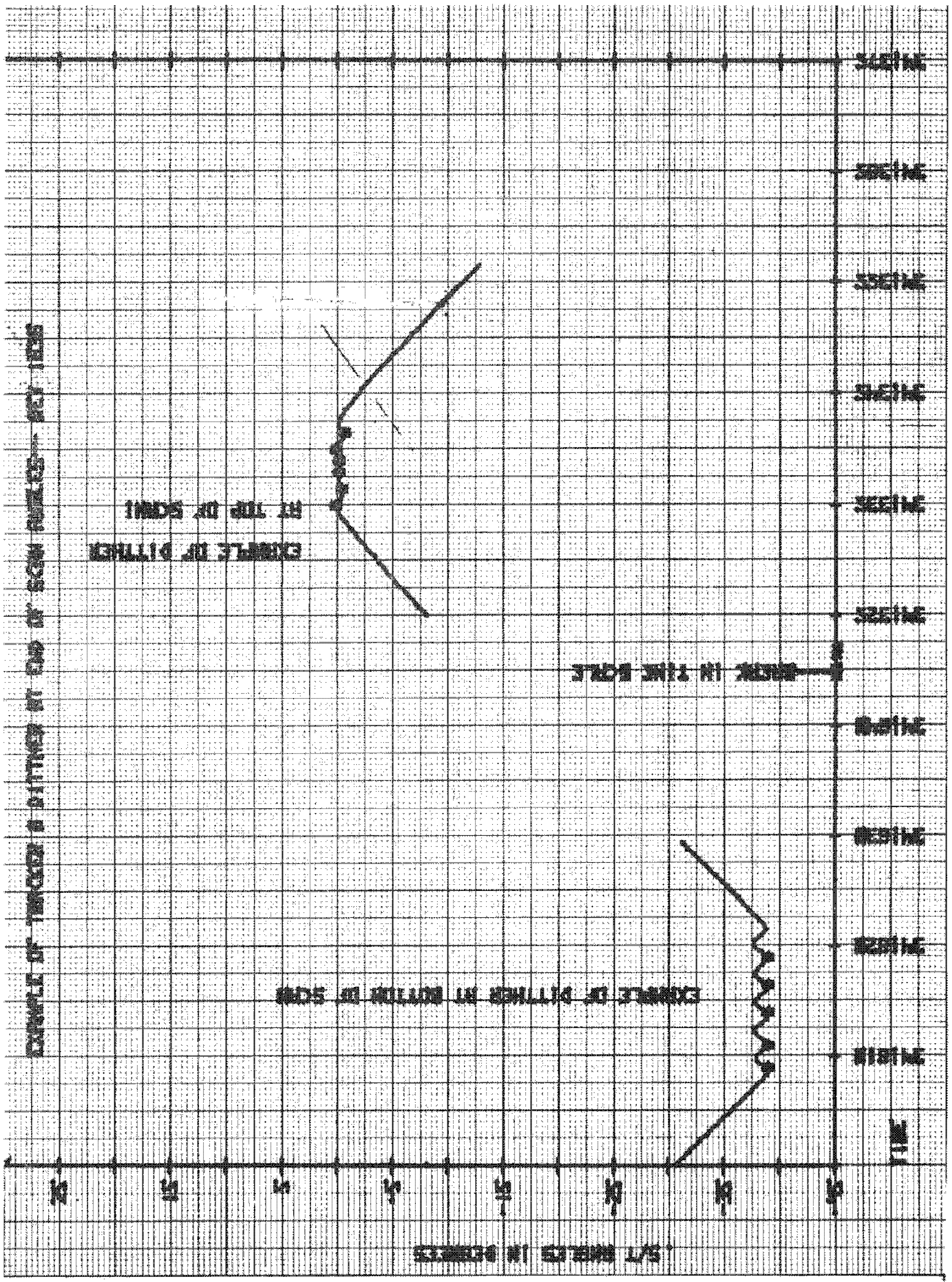

Figure 25

Example of Tracker and Dither at end of Scan Angles

3.0 SOLO TESTS - SSC

There were no Solo Tests performed by SSC on SV-8.

Approved for Release: 2025/06/18 C05137285

4.0 SOLO TESTS - MWC

4.1 MWC-1 Temperature Effects of Pressurization

Rationale

To observe the effects on pan camera pneumatics on the RV 4 automatic temperature control heater power consumption.

Procedure

The pan camera pneumatics were turned on for 130 seconds prior to perigee on Rev 1697 to obtain a nominal film path pressure. The SBA tape recorder was operated for 13 minutes prior to pressurization and for 32 minutes after the film path was pressurized.

Results

The data obtained in shown on Figure 26. No conclusions can be determined from this experiment because there was no significant change in heater power requirements when compared with nominal consumption requirements. As anticipated, the data does not show any evidence of either existing or potential thermal problems.

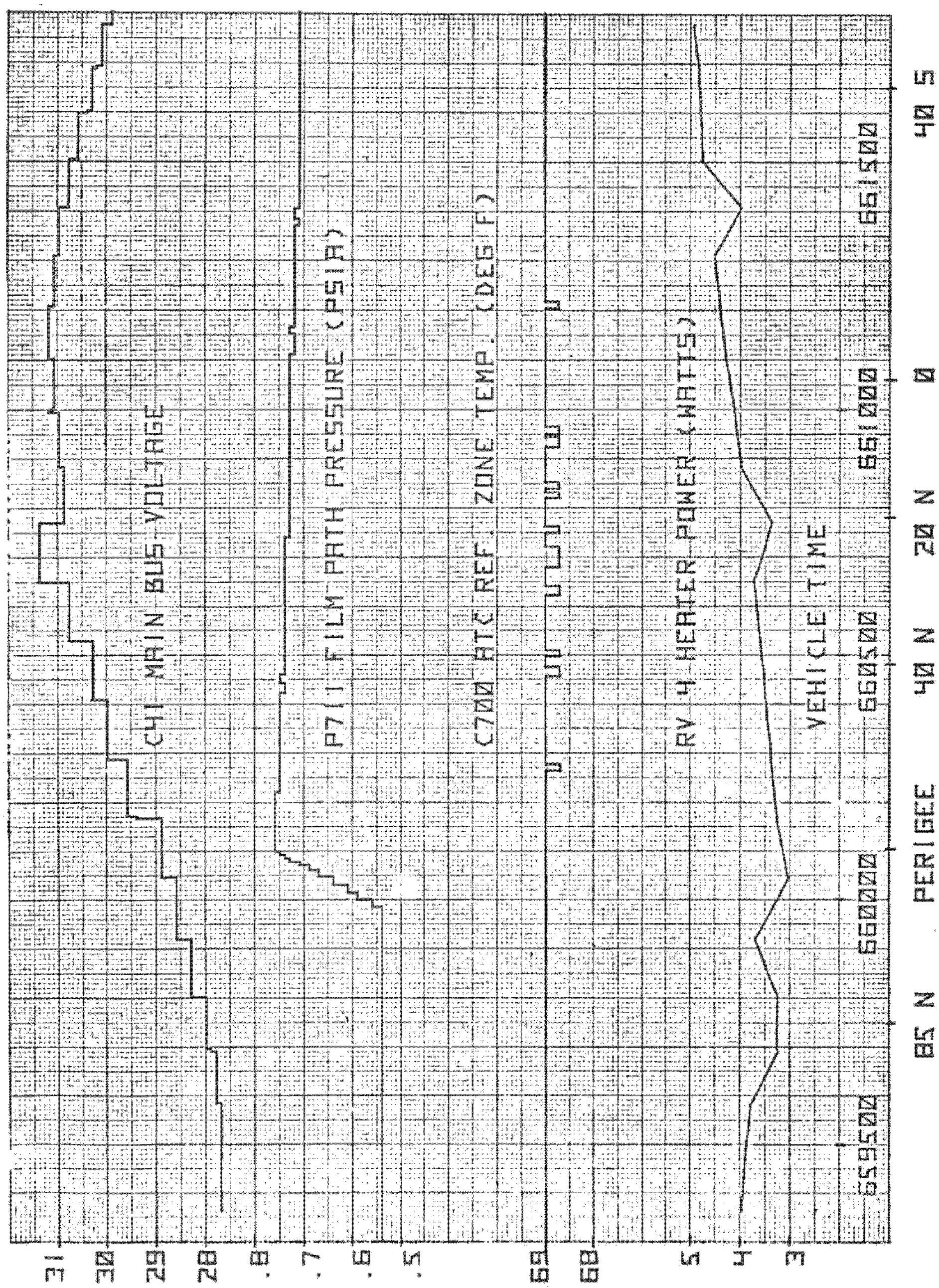

Figure 26
RV Temperature Effects Versus Pressure

5.0 SOLO TESTS - NEC

The following is a description of the test activity that was accomplished during the primary mission after the RV-5 recovery. Table XII is a summary of the NEC solo activity.

5.1 ST-1 Emergency Shutter Open Characteristics

Objective

To verify that the contingency mode of operation would have functioned if needed and to obtain thermal response data with the thermal shutter open.

Results

This experiment was not accomplished. Reference Experiment ST-3.

5.2 ST-2 Terrain Thermal Shutter Reset

Objective

To verify operation of the thermal shutter reset capability.

Results

Reference ST-3 Results.

5.3 ST-3 Verify ST Operation with Emergency Shutter Open and Reset

Objective

To verify the ST will respond when operate commands are programmed between terrain thermal shutter emergency open and reset functions.

Results

On Rev 1361 two ST operates were programmed that include commanding the thermal shutter emergency open at the start of each operate and reset at the last frame of each operate. The overlap option of 10% and 78% were also exercised. Both operates were executed. The 10% overlap was a 410 second operate.

The thermal shutter did not open with the emergency open commands on either operate. The enable and emergency open commands were added to the normal operating sequence at -3.6 and -1.6 seconds with the emergency open reset command sent 0.2 seconds after the off command.

Both the enable and emergency open commands were received and executed as evidenced by the lack of thermal shutter operation on all but the last frame operation. The thermal shutter telemetry indicated all commands were executed as programmed. (Reference Paragraph 5.6 for additional test data on the thermal shutter).

5.4 ST-4 +/-Y Stellar Capping Shutters

Objective

To verify functional operation of the stellar capping shutters.

Result

On Rev 1361 both + and - Y stellar safety capping shutters were successfully closed on the first attempt.

5.5 ST-5 Operation with One Voltage Converter Off

Objective

To determine ST operating characteristics with each converter turned off in both the normal and backup modes of operation.

Results

On Revs 1344 and 1345 four operations were executed with the following configurations:

Backup Mode Converter 2 Off
Backup Mode Converter 1 Off
Normal Mode Converter 2 Off
Normal Mode Converter 1 Off

Execution of each converter off command was verified by comparing the change in EDAP voltages. EDAP voltage comparisons are shown in Table XIII. No abnormal operation was noted when operating in either of the four indicated configurations.

With Converter 1 off, the narrow band temperature monitors indicated a drop in temperature of -0.7 to -0.9°.

During the backup mode of operation the frame time varied more than in the normal mode which was not unexpected:

Converter 1 Off range - 8.706/8.699 seconds

Converter 2 Off range - 8.733/8.710 seconds

5.6 <u>Special Terrain Thermal Shutter Emergency Open Attempts</u>

On Rev 1458, a normal emergency open sequence was executed with negative results.

On Rev 1477, a modified emergency open sequence was executed with negative results. This sequence included 20 on and off commands following the emergency open commands. The on/off commands were sent at 3 second intervals.

On Rev 1572, the system was operated for 11 cycles in the normal mode with the thermal shutter electrically reset from the emergency open sequences. Thermal shutter operation was normal. No data discrepancies were observed. The failure of the emergency open mode has been isolated to the emergency open mechanism.

TABLE XII

NEC TEST SUMMARY

Rev	Mode	Frames	FRAME TIME Calc.	FRAME TIME Actual	Comments
1327	Normal	4	8.9	8.910	Redundant electronics.
1344	Backup	5	8.9	8.733	Converter 2 off
1345	Backup	5	8.9	8.699	Converter 1 Off
1345	Normal	4	8.9	8.910	Converter 2 off
1345	Normal	4	8.9	8.909	Converter 1 Off
1361	Normal	---	---	---	+/1 Stellar capping shutter close
1361	Normal	---	8.004	---	Emergency terrain shutter open/operate/close. Overlap 78%.
1361	Normal	---	23.96	---	Emergency terrain shutter open/operate/close. Overlap 10%.
1458	---	---	---	---	Terrain thermal shutter emergency open.
1477	---	---	---	---	Emergency open pulsing technique.
1507	Normal	11	---	---	Operation normal
1572	Normal	11	---	---	Operation without thermal shutter emergency open reset.

TABLE XIII

EDAP CONVERTER SUMMARY

	BACKUP MODE		NORMAL MODE	
	Converter 1 Off, Secondary	Converter 2 Off, Primary	Converter 1 Off, Secondary	Converter 2 Off, Primary
S171	5.0	5.2	5.0	5.2
S172	-5.8	-5.6	-4.8	-4.7
S174	14.1	14.9	14.1	14.9
S175	-15.2	-15.0	-15.2	-15.0
S176	4.9	5.1	5.1	5.3
S177	-4.8	-4.7	-4.5	-4.4
S178	4.8	5.0	4.8	5.0
S181	14.3	14.8	14.3	14.9
S182	14.4	14.9	14.4	14.9
S183	4.8	5.0	4.8	5.0
S184	-15.1	-15.0	-15.1	-15.0
S185	-15.1	-15.0	-15.1	-15.0
S125	29.5	27.3	29.7	29.8
S126	27.5	27.5	27.5	27.5